3. Results

3.1. Serotonin system in the Zebrafish

To study the role of serotonin (5HT) in zebrafish development it is important to elucidate the spatial and temporal location of 5HT in early stage zebrafish embryos by using HPLC and immunohistochemistry.

3.1.1. Early stages

By HPLC, we could detect 5HT in early stages of zebrafish development namely in 8-cell embryos, blastula, gastrula, 15 somites, 1 day, and 2 day stages (Fig. 3.1). In fact, 5HT could be detected at least till 6 days old embryos. We could not find 5HT in unfertilized eggs by HPLC but after the third cleavage (8-cell stages) a 5HT signal could be detected by immunostaining using 5HT specific antibodies. Interestingly, the 5HT signal was only present in one cell of the 8 cells of this stage (data not shown). 5HT distribution in this stage is therefore asymmetrical. The same asymmetrical distribution, could be shown in the blastula with only some cells of this stage exhibiting strong and specific signals by immunostaining (Fig. 3.2).

In the gastrula, the 5HT signal after immunostaining appeared however homogenously distributed in all the cells of this stage, when compared with negative control embryos that were stained only with the secondary antibodies. The same homogenous distribution of 5HT was seen in the 15 somite stage with a stronger signal in some cells clustered in the tail of the embryos. These signals became again homogenous in the whole body of the 24 hpf and 30 hpf embryos with more strong and specific signals in olfactory bulb in the 30 hpf embryos (Fig. 3.3).

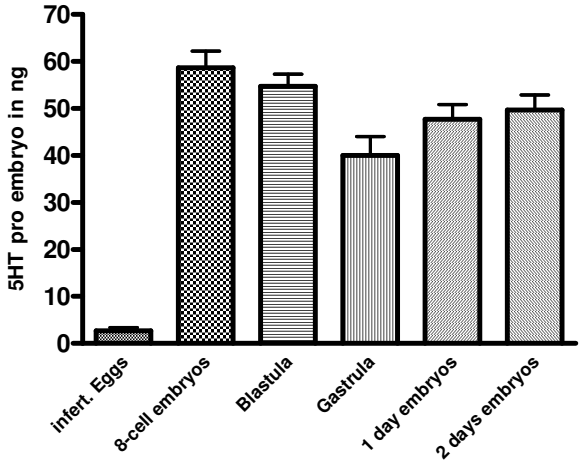

Fig. 3.1. 5HT amount in embryos of different zebrafish stages. Unfertilized eggs contain very low level of 5HT in comparison to other stages.

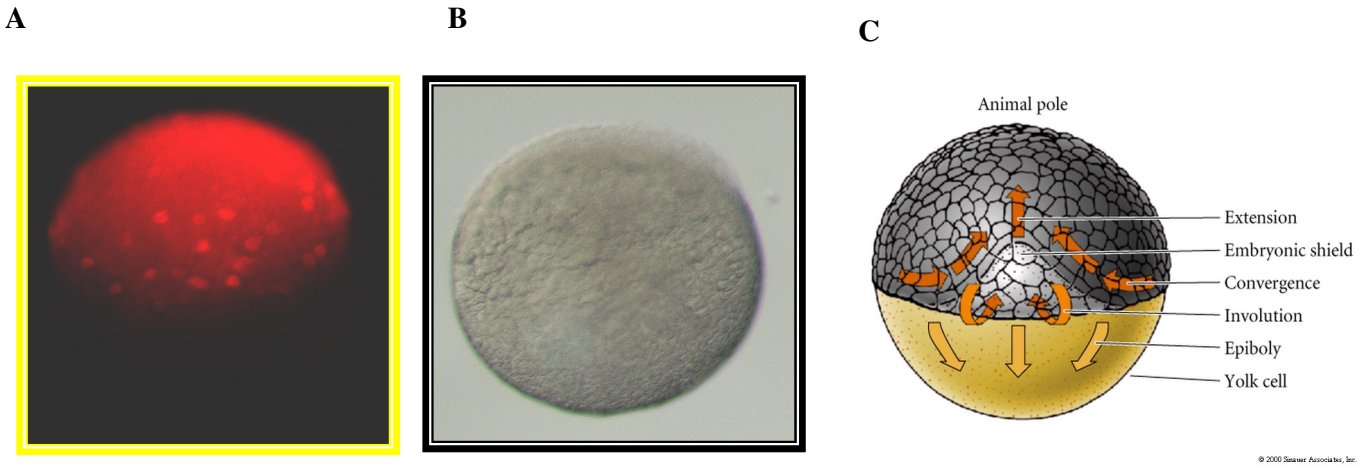

Fig. 3.2. 5HT in zebrafish blastula: (A) detected by immunostaining using 5HT antibodies. Only some cells are 5HT positive (red), (B) The same picture in phase contrast, (C) scheme of blastula.

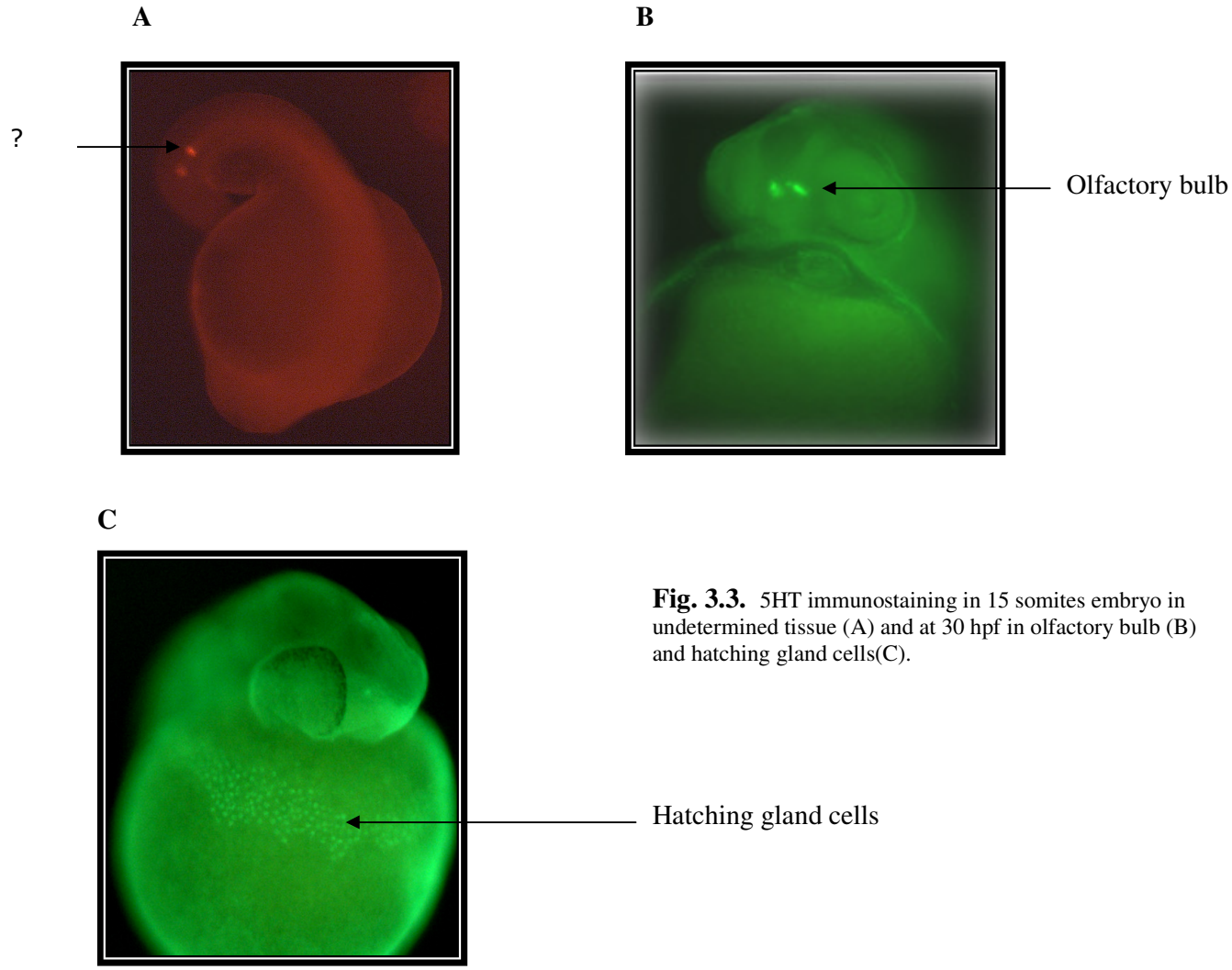

Fig. 3.3. 5HT immunostaining in 15 somites embryo in undetermined tissue (A) and at 30 hpf in olfactory bulb (B) and hatching gland cells(C).

3.1.2. Brain

In the brain of 36 hpf embryos, 5HT was detected in the hypothalamus, tuberculum and in the hindbrain rhombomers and this localization persisted till at least 6 days old embryos (Fig. 3.4).

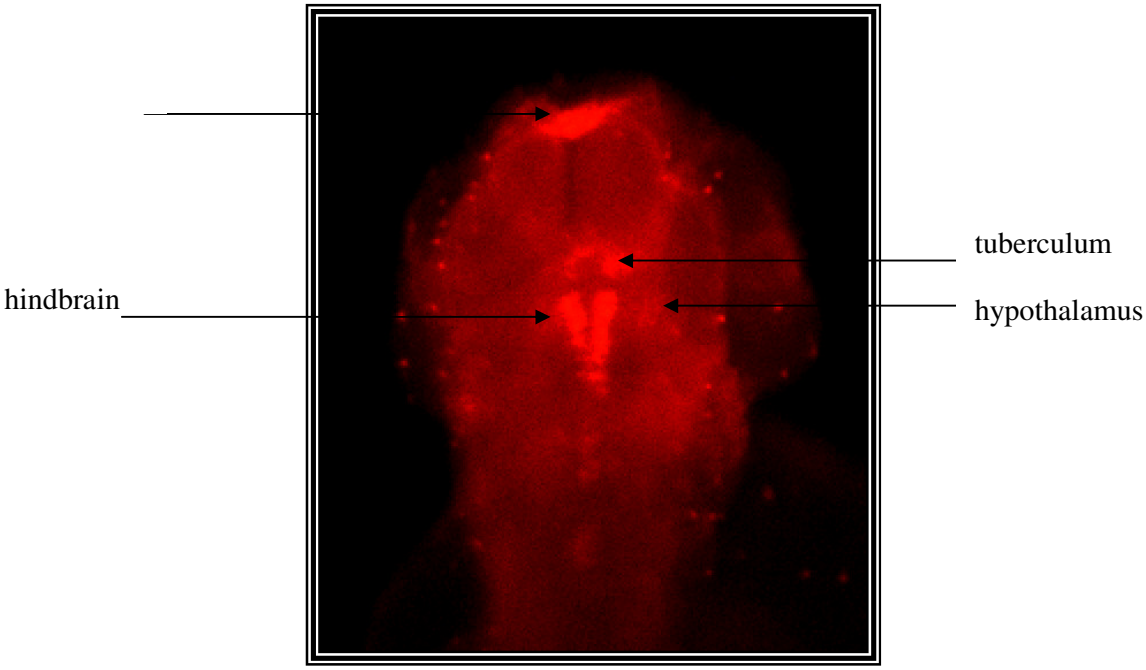

Fig. 3.4. 5HT staining in the head of 2dpf zebrafish embryo

3.1.3. 5HT single cells

In the 36 hpf stage, we could detect many single cells with strong 5HT staining, which we termed 5HT single cells (Fig. 3.5). These cells were evenly distributed in the skin of the embryos, and 5HT expression in those single cells persisted till at least 5 days old embryos. However in the 5 days old embryos, those single cells were located mainly in the pharyngeal arches, intestine, and in the dorsal root ganglion, and low in the skin, when compared with the 36 hpf stage embryos. Using the confocal microscope we could determine some of the properties of these cells (Fig. 3.6). They are located close to the gap junction of apical cells of the skin, have a diameter of 8µm and exhibit a structure similar to a hair bud at their upper surface. We were however unsuccessful to identify which kind of cells they were, since we could not detect any other marker in these cells besides 5HT. First, we thought they could be mast cells in the skin (Fig. 3.7). The staining of 5 days old embryos with alcian blue, that stains heparin in the mast cells, gave a clear blue staining of single cells in the skin. At first

sight they had the same size and the same pattern of distribution in the skin like the 5HT single cells, but by double staining the embryos with 5HT and alcian blue there was no overlap between the two cell types (Fig. 3.8). A comparable pattern of distribution of single cells in the skin can be visualized by using the dye DASPEI that labels several cell types including the hair cells in lateral line of the zebrafish. However again, both DASPEI positive cells were never 5HT positive (Fig. 3.7 and 3.9).

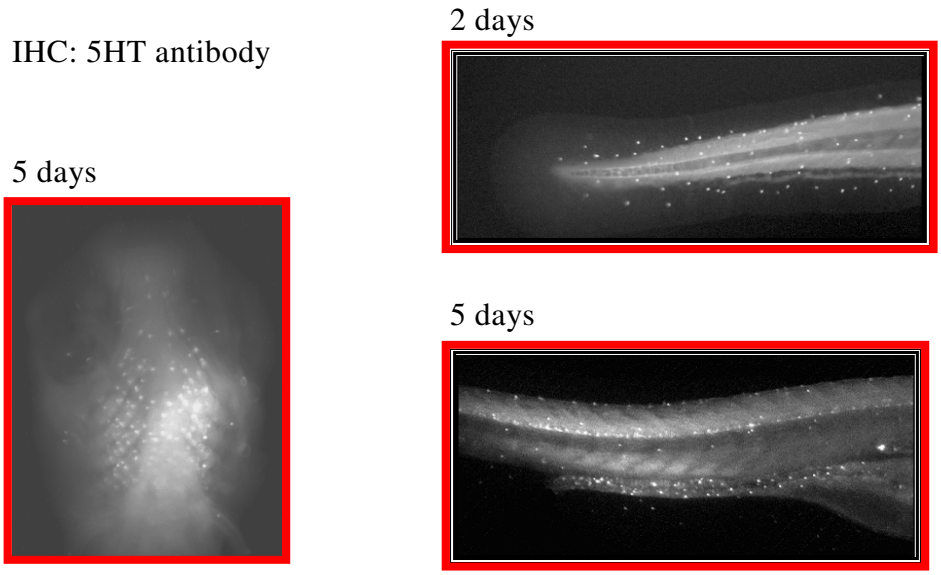

Fig. 3.5. 5HT single cells distributed in the skin of 2dpf, and intestine, dorsal root ganglion and craniofacial tissues of 5dpf zebrafish embryos

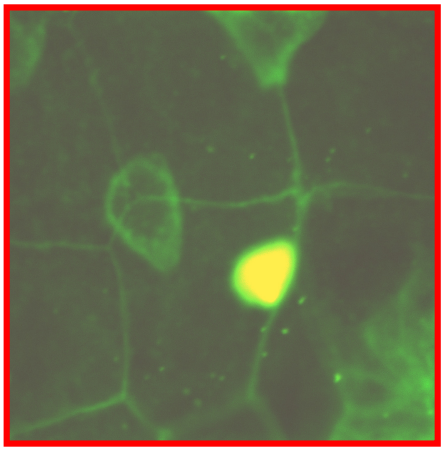

Fig. 3.6.

Confocal microscope image of a 5HT single cell (yellow) in the skin located close to the apical gap junctions (green) of the epidermal cells of claudin GFP transgenic fish.

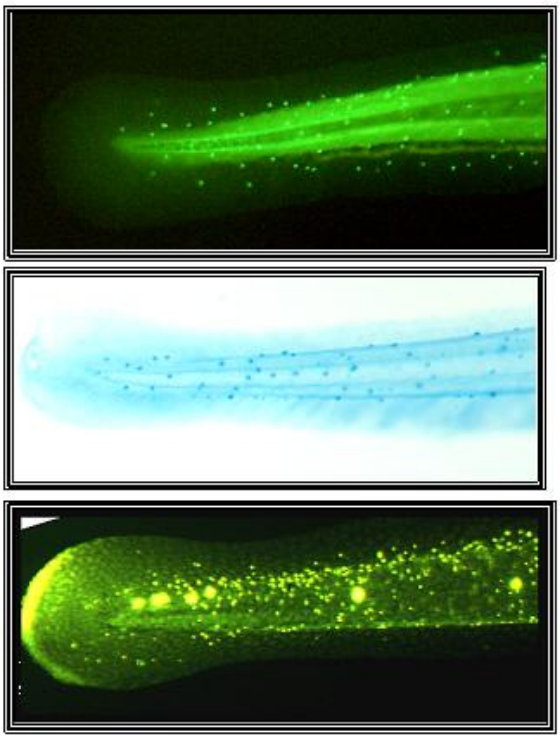

Fig. 3.7. Different kinds of single cells in the skin of the zebrafish embryos stained by 5HT antibody (green), mast cells stained by alcian blue (blue), and hair cells (yellow) stained by DASPEI.

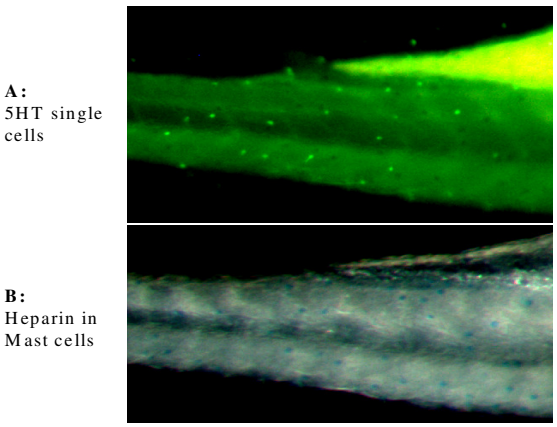

Fig. 3.8.
Double staining of the same fish embryo with 5HT antibody (green) (A) and alcian blue (blue) (B) there is no overlap between 5HT single cells and mast cells in the skin.

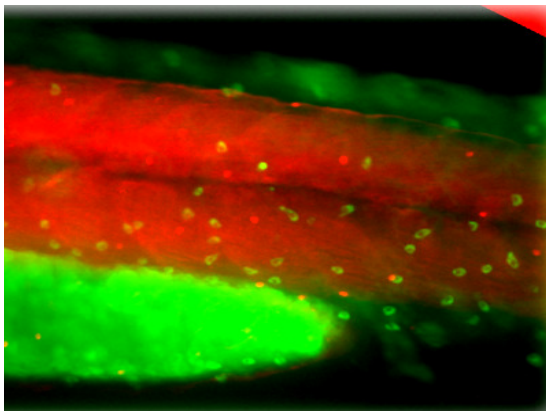

Fig. 3.9. Double staining of 2 dpf zebrafish embryo by 5HT antibody (red) and DASPEI (green), 5HT single cells in the skin are not stained by DASPEI.

Immunostaining using antibodies for the following markers: HNK1, for migrating neural crest cells; S100, for hair cells; histamine, for mast cells again gave no overlapping picture with the 5HT single cells in the skin (data not shown). During our investigation about the nature of those cells, we found by in situ hybridisation that, the transcription factor glial cells missing (Gcm2) is expressed in some cells located in pair formation on the 3-7 pharyngeal arches of 5 dpf fish but not in their midline (Fig. 3.10 A). We could not test whether those gcm2 positive cells are the same as the 5HT single cells in the pharyngeal arches (Fig. 3.10 B and C), since there is no zebrafish gcm2 antibody to do double immunostaining with 5HT.

Early, in 3 dpf embryos, we could detect 5HT single cells in the posterior pharyngeal arches, and they are located in pair formation (Fig. 3.10 D). In the same stage, we could also observe the expression of Sox9a in the posterior pharyngeal arches (Fig. 3.10 E). Sox9a is a marker for neural crest cells during their differentiation into cartilage cells. When we compare Fig.3.10 D and Fig.3.10 E, it seems that 5HT single cells in the pharyngeal arches of 3 dpf are colocalized with Sox9a positive neural crest cells, or they may be identical.

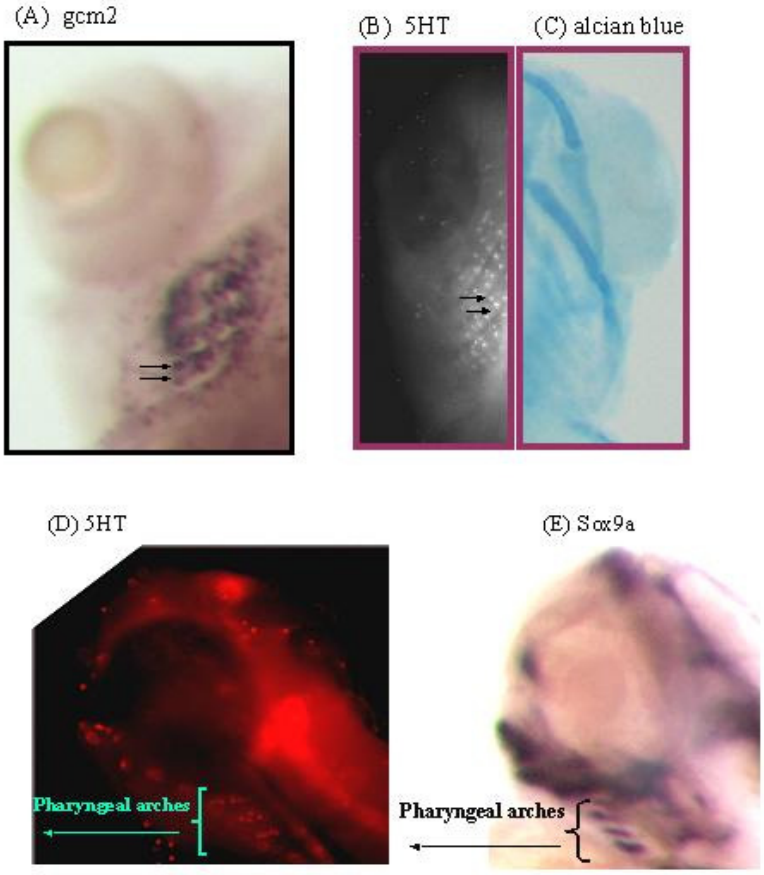

Fig. 3.10.
(A,B, and C) ventral view of pharyngeal arches of 5 dpf zebrafish embryos: stained for gcm2 (A), 5HT (B), and pharyngeal arches cartilage (C). (D andE) lateral view of 3dpf embryos: stained for 5HT(D), and Sox9a (E) (see text).

According to the morphology of 5HT single cells in the skin, and the fact that they carry a hair-like structure on their surface, we tested them for their sensitivity against aminogylcosides, that induce cell-death in lateral line hair cells. After exposure of the embryos to aminoglycoside and then staining them with the 5HT antibody, there was no cell-death effect on 5HT single cells, while the lateral line hair cells disappeared, as shown by DASPEI staining (data not shown).

3.1.3.1. How 5HT single cells get serotonin?

We wanted to find out, whether 5HT single cells can synthesize 5HT, or whether they take it up by SERT. However none of the commercial antibodies for TPH can cross react with the zebrafish TPH isoforms, except a human TPH2 antibody (Abcam), which gave signals only in the pineal gland and in the preoptic area of 2 days old zebrafish embryos. By in situ hybridisation experiments, using mRNA antisense probes of the three TPH isoforms TPHD1, TPHD2, and TPH2 we could not detect any expression of the three isoforms in the 5HT single cells. The same negative results were obtained by using riboprobes for zebrafish SERT.

Additionally, we performed a **pharmacological loss-of-function test** with two inhibitors of the 5HT system: parachlorophenylalanine (pCPA), a specific inhibitor of TPH and, fluoxetine, a specific blocker of SERT.

One cell-embryos were either incubated with pCPA or fluoxetine (10 µM, 100 µM, 1mM, 10mM, and 50mM) or injected with the same concentrations of pCPA or fluoxetine and incubated further with pCPA or / and fluoxetine in the water until the fishes were 5 days old. Different stages of these fishes were selected for serotonin staining. We could detect no difference between them and the controls, nor could we see any effect of pCPA or fluoxetine on the zebrafish by this protocol (data not shown). Then we used the **genetic loss-of-function test**, i.e. the injection of specific morpholino antisense oligonucleotides against the mRNAs of TPHD1 and TPH2. Only the TPH2 morphant fish showed significant reduction of 5HT signals in single cells in the skin of 2 days old fish and in the pharyngeal arches of 5 days old fish (Fig. 3.11 and 3.24). In the brain of 2 days old fish there was a strong reduction of 5HT signals in the hypothalamus and in the olfactory bulb. However, we could only detect a slight reduction in 5HT immunoreactivity in the raphe nucleus of the 2 days old TPH2 antisense morphants when compared with the wild type. It is needed to be mentioned that this genetic loss-function test produces only a knock down of the targeted gene with limited efficiency and just for a maximum of 5 days and not a complete knock out of the targeted gene.

On the other hand, we could not detect any reduction of 5HT single cells in the intestine of 5 days old embryos of the TPHD1 or TPH2 morpholino knock-down fish in comparison to the wild type. The double knock down fish for TPHD1 and TPH2 died before they reach the gastrulation stage. It is known that in the adult mammals both TPH isoforms are expressed in the intestine. TPH1 is expressed intensively in the enterochromaffin cells, and TPH2 in the enteric nervous system (Gershon 2005). Maybe 5HT single cells in the zebrafish are precursors for both tissues, and in case one of them decrease the other will increase, or may be at this late stage there is no inhibition effect of the morpholino.

Fish injected with TPHD1 morpholino antisense oligonucleotides showed only a reduction in 5HT signals in the pineal gland. This morpholino had no effect on 5HT single cells, which still exhibited the same signal intensity of 5HT as the wild type.

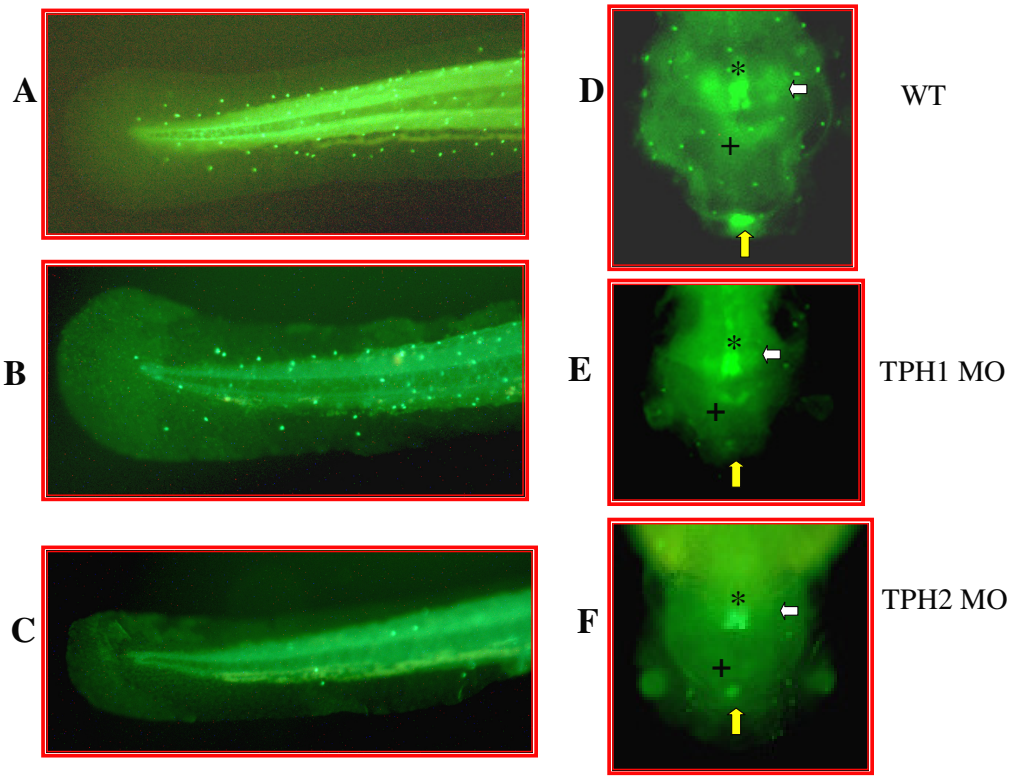

Fig. 3.11. 5HT staining in 2dpf embryos. (A,B,C) lateral view; (D,E,F) dorsal view of the head. Wild type (A,D); TPHD1 morphants (B,E); TPH2 morphants (C,F). *: raphe nucleus, +: tuberculum,: ⇨ hypothalamus , ➡: pineal gland. In comparison to the wild type, TPHD1 morphants exhibit reduction in 5HT signal only in the pineal gland, while TPH2 morphants show reduction in 5HT signals in 5HT single cells, tuberculum, hypothalamus and slightly in the raphe nucleus (see text).

3.1.3.2. The origin of 5HT single cells

Due to defects in many neural crest cell derived tissues in the TPH2 morphants, we questioned if these 5HT single cells were also neural crest derived. Therefore we decided to delete neural crest cells by specific morpholino antisense oligonucleotides targeting an important gene in the early development of these cells. As first candidate gene we selected Foxd3. Recently (Lister et.al. 2006; Stewart et al. 2006) mutant fish for this gene were shown to have similar phenotypic defects in craniofacial elements and iridophores like the TPH2 morphants (3.4.2.1, 3.4.2.2). We injected the one-cell embryo with specific Foxd3 morpholino antisense oligonucleotide and confirmed the decreased Foxd3 protein biosynthesis by staining 5 and 10 somites stage embryos with a zebrafish specific Foxd3 antibody. This showed, that the Foxd3 protein signal disappeared in neural crest cells (Fig. 3.12). To study the effect of the Foxd3 gene on the 5HT single cells, we stained different stages of the Foxd3 morphants with the 5HT antibody. In early phases, when the 5HT single cells appear on the skin of the 36 hpf old embryos, the Foxd3 morphants showed no difference to the wild type. The skin of Foxd3 morphants contained similar amount of 5HT cells as the controls (data not shown). However in later stages, like in 5 days old embryos, when the 5HT single cells appeared in the pharyngeal arches, dorsal root ganglion and intestine, the Foxd3 morphants showed a strong reduction of 5HT cells in these three tissues in comparison to the wild type (Fig. 3.13). The skin still contained the same amount of 5HT cells like the skin of 5 days old wild type embryos. It is however known that the neural crest cells migrate from the dorsal neural tube in two directions, the first group migrates dorso-ventrally towards the craniofacial area, dorsal root ganglia and intestine tissues. This group maybe dependent on Foxd3. The second crest cell group migrates in the dorsal-lateral direction into the skin to produce melanocytes.

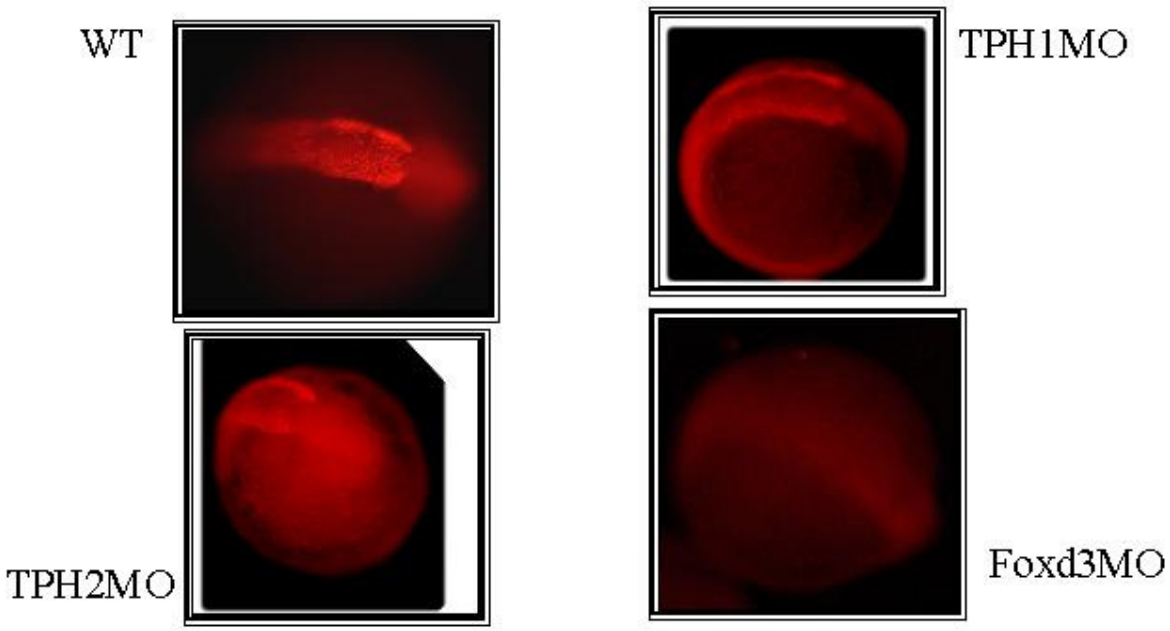

Fig. 3.12. Whole mount immunohistochemistry with Foxd3 antibodies in 5 somites zebrafish embryos. Foxd3 protein disappeared only from Foxd3 morphants (Foxd3MO).

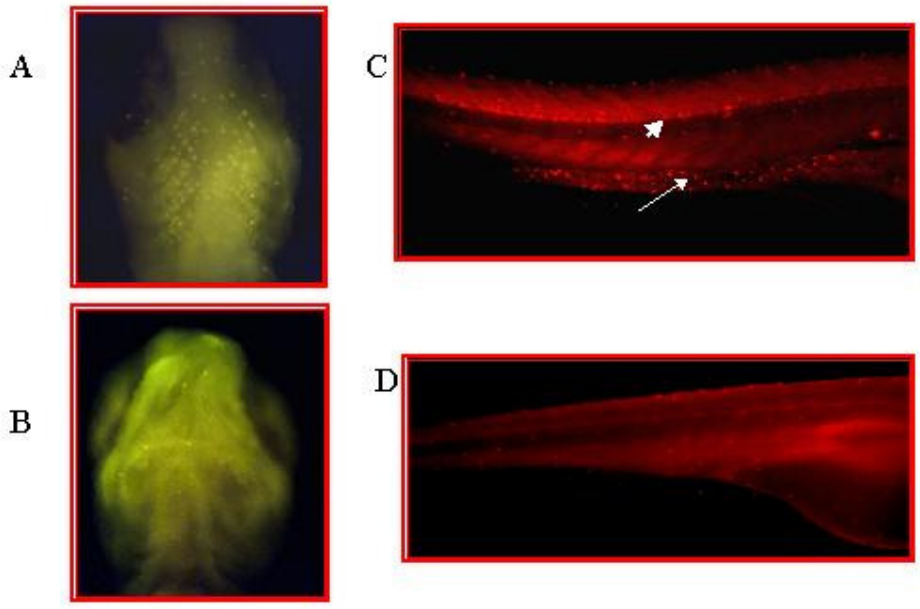

Fig. 3.13. 5HT single cells in the pharyngeal arches of 5 days old zebrafish embryo (A), as well as in intestine (arrow), and dorsal root ganglion (arrow head) (C). In Foxd3 morphants (B) and (D), these cells are missing in pharyngeal arches, intestine and dorsal root ganglia.

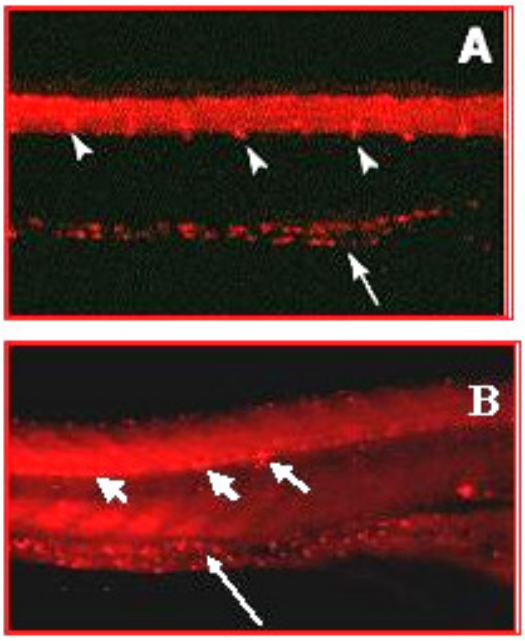

Fig. 3.14. 5HT single cells in the intestine (arrow) and in dorsal root ganglia (arrow head) of 5 days old zebrafish embryos labelled with 5HT antibody (B). (A) Neurons in the intestine (arrow) and the dorsal root ganglia (arrow head) of the same age labelled with Hu antibody (Lister et al. 2006)

Dutton et al. (2001) reported about the *colourless* zebrafish mutant and could identify the transcription factor Sox10 as essential factor in the development of the neural crest derived melanocytes in the skin. The transcription factor Sox10 is expressed in pre-migratory neural crest cells at 12 hpf, and down regulated when the neural crest cells start to migrate.

We injected one-cell embryos with Sox10 morpholino antisense oligonucleotides (Whitlock et al. 2005). By immunostaining, we found that 5HT single cells signal in the skin of 2 dpf almost completely disappeared (Fig. 3.16). This observation clarified that 5HT single cells in the skin originate from neural crest cells regulated by Sox10 and not by Foxd3. However the effect of Sox10 deletion on 5HT cells in the brain and pineal gland was surprising (Fig. 3.16). 5HT cells in the raphe nucleus were reduced and there was a change in their location, the residual cells located asymmetrical in comparison to the symmetrical 5HT cells in the raphe nucleus of the brain of the wild type. The 5HT signal in the pineal gland and hypothalamus also disappeared, while the amount of 5HT in the tuberculum was slightly increased and changed its location.

Fig. 3.15. Wild type (A) and Sox10 morphant (B) zebrafish 2 dpf. Melanocytes are absent in the skin of the morphant, while the retinal epithelium, which is not neural crest derived is still filled with melanin.

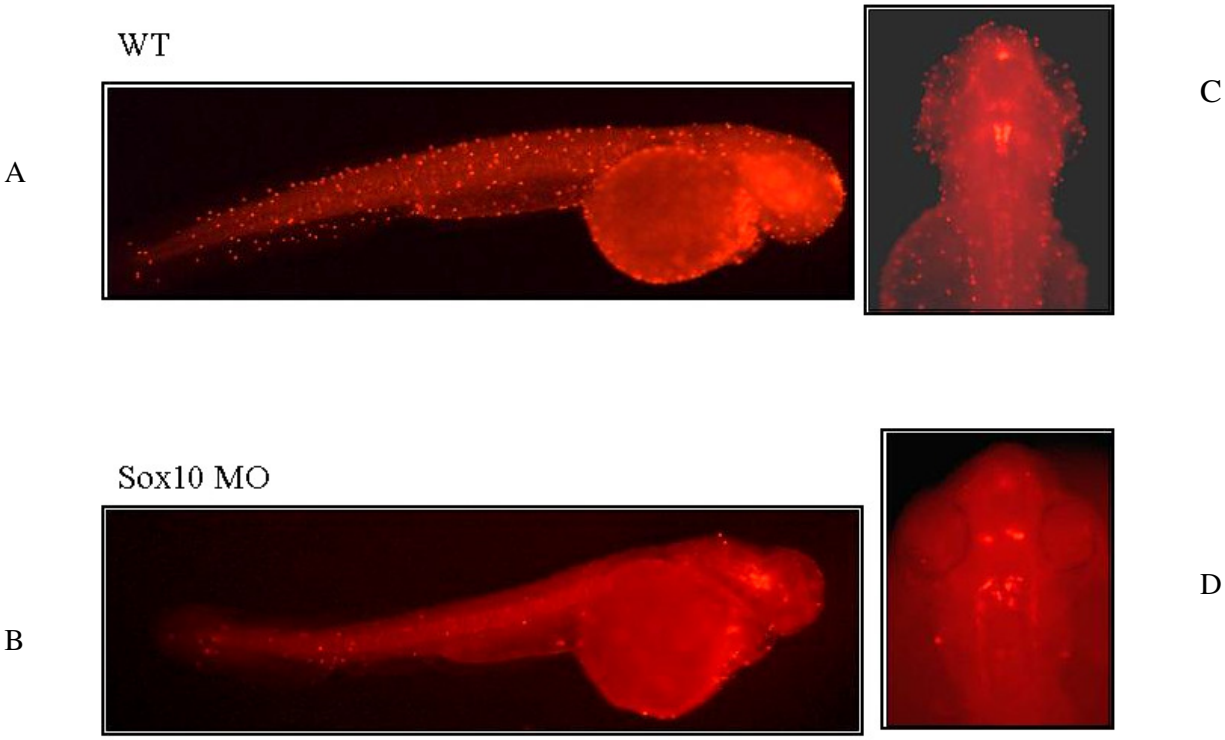

Fig. 3.16. Immunostaining with 5HT antibody of 2 dpf wild type zebrafish embryos (A) and (C) and Sox10 morphants (B) and (D). Lateral view (A) and (B), dorsal view (C) and (D). 5HT single cells in the skin of Sox10 morphants are almost absent (B) in comparison to the wild type (A). 5HT cells in raphe nucleus of Sox10 morphants are located asymmetrically, in the pineal gland and hypothalamus the 5HT signal is strongly reduced and in the tuberculum slightly increased with a change in its location (D) in comparison to the wild type.

3.2. Cloning and sequencing of TPH isoforms in the zebrafish

We screened the zebrafish data base using cDNA fragments from the conserved domains of mammalian TPH1 to look for TPH genes in the zebrafish. At first we could find two different cDNA fragments with around 600 bp, one isolated from the ovary and the other from the brain of adult fish. By using RT-PCR, we amplified the two fragments. Later, a small fragment of a third zebrafish TPH isoform was published by others (Ballipani et al. 2002) different from what we found in GenBank. By using the blast algorithm we could identify the full length cDNA of the three TPH isoforms in the zebrafsh: 1) TPHD1 accession number (AF548566), 2) TPHD2 accession number (AY616135), and 3) TPH2 accession number (AY616134). A comparison of the amino acid sequences of the three zebrafish TPH isoforms with the two human TPH isoforms is shown in Table 1 and in Fig. 3.17.

SeqA	Name	Len(aa)	SeqB	Name	Len(aa)	Score
1	hTPH1	444	2	hTPH2	490	70
1	hTPH1	444	3	drTPHD1	471	75
1	hTPH1	444	4	drTPHD2	480	75
1	hTPH1	444	5	drTPH2	500	69
2	hTPH2	490	3	drTPHD1	471	65
2	hTPH2	490	4	drTPHD2	480	67
2	hTPH2	490	5	drTPH2	500	77
3	drTPHD1	471	4	drTPHD2	480	78
3	drTPHD1	471	5	drTPH2	500	64
4	drTPHD2	480	5	drTPH2	500	64

Table 1. Comparison of amino acid sequences of all TPH isoforms from human and zebrafish. TPH1 from human is more similar to TPHD1 and TPHD2 from zebrafish, while the human neural isoform TPH2 is more similar to TPH2 from zebrafish.

```
drTPHD1          -----MYSSKSDGPRRGRSFDSMNLGMTLEEKQLNNEMNKSAFTKIEENKDNKTESS--- 52
drTPHD2          -----MLSNKLDGPRRGRSFDSINK--NYEEKLLSNELRKTTFHKTDENKD-KKLSS--- 49
hTPH1            ---------------------------------------------MIEDNKENKDHSL--- 13
hTPH2            MQPAMMMFSSKYWARRGFSLDSAVP--EEHQLLGSSTLNKPNSGKNDDKGNKGSSKREAA 58
drTPH2           MQPAMMMFSSKYWARRGLSLDSAMY--DQQHLA-SSMLRRTSFNRIDERPDKEEQK--ST 55
                                                                  ::. :    .

drTPHD1          -ETGRAAVVFSLKNEVGGLVKALKLFQENHVNLVHIESRKSKRRNSEFEIFVDCDSNREQ 111
drTPHD2          -KREHAAIVFSLKNEVGGLVKALKLFQDNQVNLLHIESRKSRRRNSELEVLVDCDSDRET 108
hTPH1            -ERGRASLIFSLKNEVGGLIKALKIFQEKHVNLLHIESRKSKRRNSEFEIFVDCDINREQ 72
hTPH2            TESGKTAVVFSLKNEVGGLVKALRLFQEKRVNMVHIESRKSRRRSSEVEIFVDCECGKTE 118
drTPH2           HDLGKLAVIFSLKNEVGFLVKALRLFQEKHVNLAHIESRRSKRLTNEIEIYAECNCTKKE 115
                  .  : :::******** *:***::**::::**: *****:*:* ..*.*: .:*:  :

drTPHD1          LHEIIQLLRKHVNVVEMDAPDNRLAEESE------------MENVPWFPKKISDLDKCA 158
drTPHD2          LKEIVQLLRKQTSIIAMNSPDKFWTPASD------------LAEVPWFPKKISDLDKSA 155
hTPH1            LNDIFHLLKSHTNVLSVNLPDNFTLKEDG------------METVPWFPKKISDLDHCA 119
hTPH2            FNELIQLLKFQTTIVTLNPPENIWTEEEE------------LEDVPWFPRKISELDKCS 165
drTPH2           FNELVQHLKDHVNIVSYNTPQHVWSAETECLDCVCVLGGLPDGEGIPWFPQKISELDQCS 175
                 ::::.: *: :..::  : *::                      :****:***:**:.:
```

```
drTPHD1         NRVLMYGSDLDADHPGFKDNVYRKRRKYFADLAMSYKHGDPIPRIEFTEEEVKTWGVVFR 218
drTPHD2         CRVLMYGSELDADHPGFKDNVYRKRRKYFADLAMSYKHGDPIPHVEFTEEEVKTWGVVFR 215
hTPH1           NRVLMYGSELDADHPGFKDNVYRKRRKYFADLAMNYKHGDPIPKVEFTEEEIKTWGTVFQ 179
hTPH2           HRVLMYGSELDADHPGFKDNVYRQRRKYFVDVAMGYKYGQPIPRVEYTEEETKTWGVVFR 225
drTPH2          HRVLMYGSELDADHPGFKDKVYRQRRKYFVEVAMNYKFGQPIPRIEYTAEEVKTWGVVYR 235
                 *******:**********:***:*****.::**.**.*:***::*:* ** ****.*::

drTPHD1         ELNKLYPSHACREYLKNLPLLIKHCDSREDNIPQLEDVSRFLKERTGFTIRPVAGYLSPR 278
drTPHD2         ELNKLYPTHACREYLQNLPLLSQFCGYREDNIPQLEDVSNFLRERTGFTIRPVAGYLSPR 275
hTPH1           ELNKLYPTHACREYLKNLPLLSKYCGYREDNIPQLEDVSNFLKERTGFSIRPVAGYLSPR 239
hTPH2           ELSKLYPTHACREYLKNFPLLTKYCGYREDNVPQLEDVSMFLKERSGFTVRPVAGYLSPR 285
drTPH2          ELTKLYPTHACREYLKNLPLLTKHCGYREDNIPQLEDVSLFLRERSGFTVRPVAGYLSPR 295
                **.****:*******:*:*** :.*. ****:******* **:**:**::**********

drTPHD1         DFLAGLAFRVFHCTQYVRHSSDPLYTPEPDTCHELLGHVPLLAEPSFAQFSQEIGLASLG 338
drTPHD2         DFLAGLAFRVFHCTQYVRHSSDPLYTPEPDTCHELLGHVPLLAEPSFAQFSQELGLASLG 335
hTPH1           DFLSGLAFRVFHCTQYVRHSSDPFYTPEPDTCHELLGHVPLLAEPSFAQFSQEIGLASLG 299
hTPH2           DFLAGLAYRVFHCTQYIRHGSDPLYTPEPDTCHELLGHVPLLADPKFAQFSQEIGLASLG 345
drTPH2          DFLAGLAYRVFNCTQYIRHSTDPLYTPEPDTCHELLGHVPLLADPKFAQFSQEIGLASLG 355
                ***:***:***:****:**.:**:********************:*.*******:******

drTPHD1         ASDDSIQKLATCYFFTVEFGLCKQEGKLRAYGAGLLSSISELKHALSGNARILPFDPNVT 398
drTPHD2         ASDDAVQKLATCYFFTVEFGLCKQEGSLRAYGAGLLSSISELKHSLSDSAKILPFEPKVT 395
hTPH1           ASEEAVQKLATCYFFTVEFGLCKQDGQLRVFGAGLLSSISELKHALSGHAKVKPFDPKIT 359
hTPH2           ASDEDVQKLATCYFFTIEFGLCKQEGQLRAYGAGLLSSIGELKHALSDKACVKAFDPKTT 405
drTPH2          ASDEDVQKLATCYFFTIEFGLCKQDGQLRVYGAGLLSSIGELRHALSDKATVKVFDPKTT 415
                **:: :**********:*******:*.**.:********.**:*:**. * :  *:*: *

drTPHD1         CKQECIITTFQDVYFMSDSFEEAKVKMREFAKTIKRPFSVRYNPYTQSVDVLKDT-TLNN 457
drTPHD2         CKQECLITTFQDVYFVSESFEEAKCRMREFAKTIQRPFSLRYNPYTQSVCVLKDMPSIND 455
hTPH1           CKQECLITTFQDVYFVSESFEDAKEKMREFTKTIKRPFGVKYNPYTRSIQILKDTKSITS 419
hTPH2           CLQECLITTFQEAYFVSESFEEAKEKMRDFAKSITRPFSVYFNPYTQSIEILKDTRSIEN 465
drTPH2          CYQECLITTFQDVYFVSESFEEAKEKMREFAKSIKRPFSVYYNPYTQSIDLLKDTRSIEN 475
                * ***:*****:.**:*:***:** :**:*:*:* ***.: :****:*: :***  :: .

drTPHD1         VVEELN-MTGHLGDA---------- 471
drTPHD2         VVEELRHELDIVGDALCRLSTHLGV 480
hTPH1           AMNELQHDLDVVSDALAKVSRKPSI 444
hTPH2           VVQDLRSDLNTVCDALNKMNQYLGI 490
drTPH2          VVQDLRSDLTTVCDALGKMNKYLGI 500
                .:::*.     : **
```

Fig. 3.17. Comparison of amino acid sequences of all TPH isoforms from human and zebrafish. "*" the residues in that column are identical in all sequences,":" conserved substitutions have been observed , "." semi-conserved substitutions are observed (see text).

3.3. Expression pattern of TPH isoforms in the zebrafish embryos

3.3.1. TPHD1

mRNA expression of TPHD1 was detectable by in situ hybridization at 24 hpf in the pineal gland, where it persists at least until 6 dpf (Fig. 3.18). This correlates with 5HT immunoreactivity which started 6 hours later, at 30 hpf. Serotonin is known as a precursor of melatonin biosynthesis in the pineal gland. TPHD1 mRNA could be detected also in the lens of 36 hpf old embryos. This correlates with the immunostaining of 5-OHTrp in the lens of 2 days old embryos (data not shown). 5-OHTrp is the direct product of Trp hydroxylation by TPH. We could not observe 5HT signals in the lens, maybe due to the absence of AAAD, that

decarboxylates 5-OHTrp to produce 5HT, or the possibility that 5HT may be quickly processed into melatonin to regulate the circadian clock in the retina (Appelbaum et al. 2006).

.

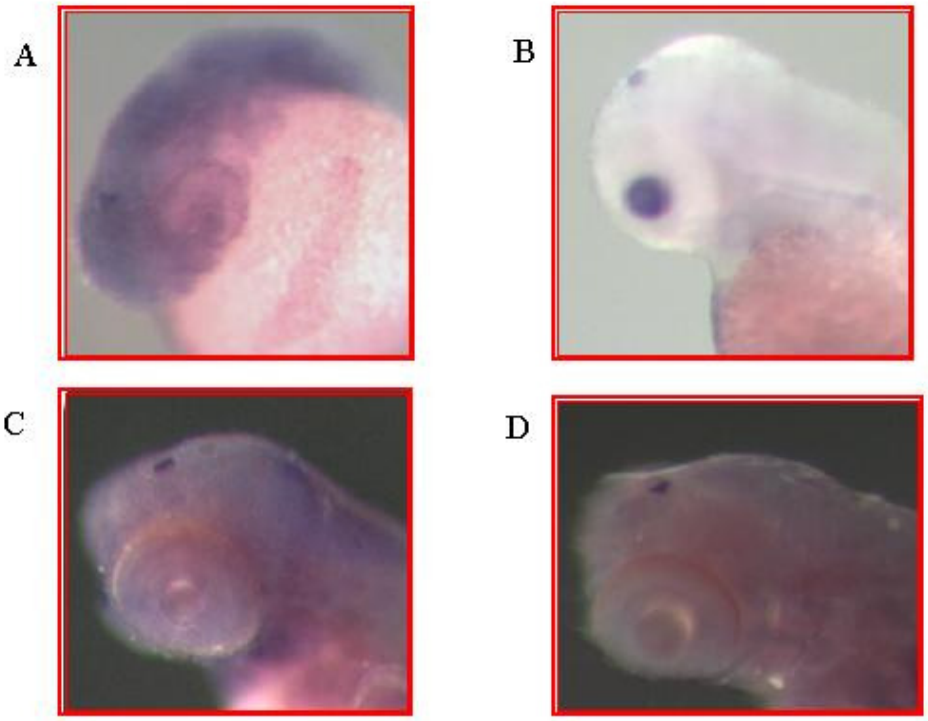

Fig. 3.18. in situ hybridization with TPHD1 riboprobe of (A) 1dpf; (B) 2dpf; (C) 4dpf; (D) 6dpf zebrafish embryos. TPHD1 expression is mostly restricted to the pineal gland at least till 6dpf.

3.3.2. TPHD2

After the successful cloning of the full length cDNA of TPHD2, we had difficulties to detect by in situ hybridization the expression pattern of TPHD2 in the different embryo stages (one-cell- , 8-cell-embryos, blastula, gastrula, 10 somites, 24 hpf, 32 hpf, 36 hpf, 2 dpf, 3 dpf, 4 dpf, 5 dpf, and 6dpf). It was not possible to observe any specific signal using five different antisense riboprobes, even in the preoptic area of the ventral diencephalon where TPHD2 expression has been reported previously (Bellipanni et al. 2002). However, we could identify a positive immunoreactivity in the ventral preoptic area of 2 dpf embryos using an antibody against hTPH2 (Fig. 3.19). Since no signal in the preoptic tissues could be detected by in situ hybridization with TPHD1 or TPH2 antisense riboprobes, and since the hTPH2 amino acid sequence (50-104 aa), that was used as antigen to produce the antibody, is similar to all three zebrafish TPH isoforms, we assume that the immunoreactivity may represent TPHD2.

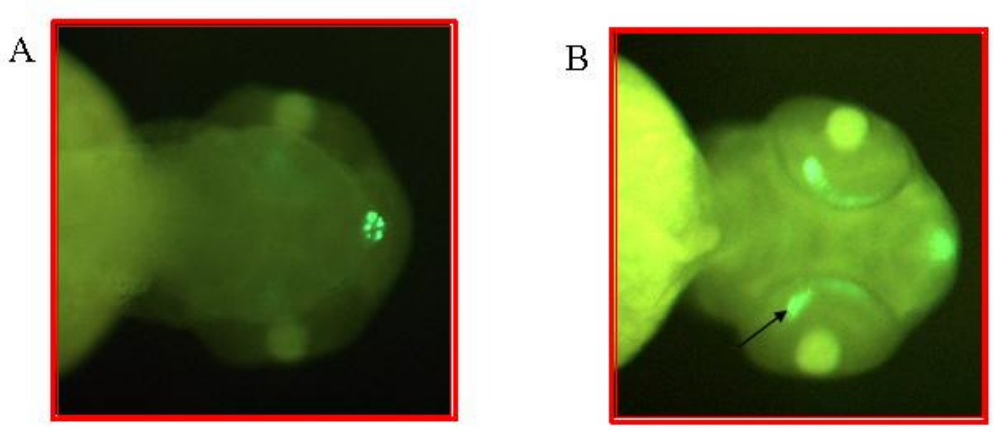

Fig. 3.19. Immunostaining with hTPH2 antibodies of 2dpf zebrafish embryos. (A) dorsal view shows the pineal gland; (B) ventral view shows the pineal gland and also positive signal in the preoptic tissue (arrow) probably detecting the expression of the TPHD2 isoform.

3.3.3. TPH2

Zebrafish TPH2 is located in linkage group 18, and we could detect its mRNA by in situ hybridization only up to 36 hpf in bilateral longitudinal columns in the anterior hindbrain (Fig 3.20 B), which correspond to raphe neurons showing 5HT immunoreactivity (Fig.3.4). Whereas in the adult zebrafish serotonergic neurons were divided into dorsal (B6-B7) and ventral clusters (B1-B2) (Kaslin and Panula 2001), during the larval stages these neurons instead form rostral and caudal cluster (Teraoka et al. 2003). We should mention here that 5HT single cells in the skin become immunoreactive at the same stage as raphe neurons showing 5HT immunoreactivity, even if we could not detect TPH2 in 5HT single cells in the skin (see also 3.1.3.1).

In contrast to mammals, TPH2 can be also detected by in situ hybridization in the pineal gland of the zebrafish larvae. Zebrafish express both TPH isoforms, TPHD1, at 24 hpf, and TPH2, later, at 36 hpf. It is known that, the pineal gland of the zebrafish contains two different epiphysial cell types: photoreceptors and projection neurons (Cau and Wilson 2003). Further investigations are necessary to confirm if both TPH isoforms are expressed in those different cells separately or in the same cells together. We could not detect TPH2 in the hypothalamus or in the tuberculum.

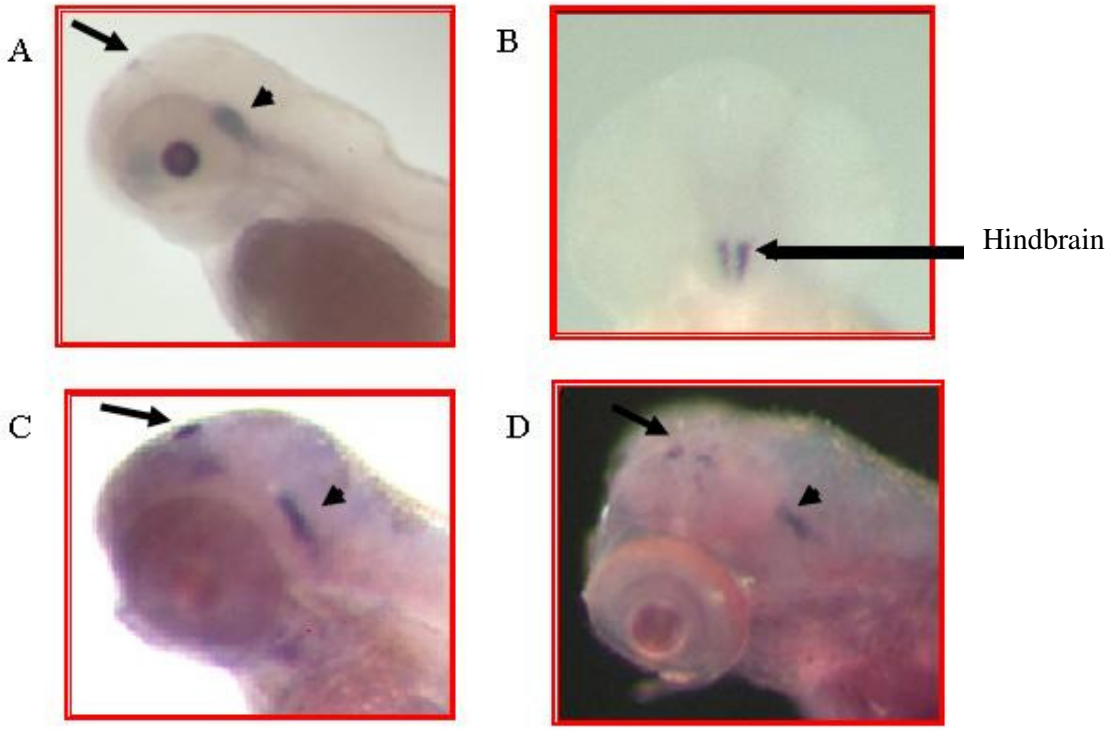

Fig. 3.20. in situ hybridization with TPH2 riboprobe. (A,B) 2dpf ; (C) 4dpf; (D) 6dpf zebrafish embryos. (A,C,D) lateral view showing TPH2 expression in hindbrain (arrow head) and pineal gland (arrow). (B) dorsal view showing TPH2 expression in hindbrain (arrow).

3.4. Phenotyping the TPHD1 and TPH2 knockdown zebrafish embryos

To test the role of serotonin in the development of zebrafish, we injected the morpholino antisense oligonucleotides for TPHD1 and TPH2 separately into the yolk of 1-cell stage embryos to knockdown both TPH isoforms, and then incubated the fish till they are 6 days old.

3.4.1. TPHD1 morphants

From their overall morphology, TPHD1 morphants were growing normal at least until they are 6 days old (Fig. 3.21).

3.4.2. TPH2 morphants

Also TPH2 morphants had a normal morphology until 48 hpf. However by the third day the shape and the size of the TPH2 morphants begun to differ from the wild type, mainly they became shorter and more rounded as shown in Fig. 3.21.

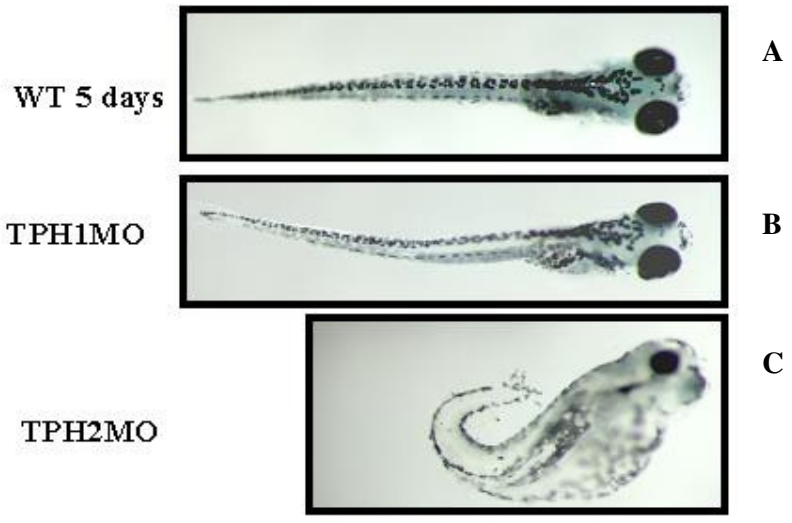

Fig. 3.21. Change in the external form and size of TPH2 morphants (C) compared to wild type (A) and TPHD1 morphants (B) at 5dpf.

3.4.2.1. Ventral pharyngeal arches

Alcian blue staining

We examined the cartilage of pharyngeal arches of the morphants using alcian blue staining. Larvae injected with only TPH2 morpholinos showed greatly reduced cartilage in the pharyngeal archs compared with uninjected controls and those injected with TPHD1 morpholinos (Fig. 3.23). Specifically, all the five posterior pharyngeal aches

(ceratobranchials) (cb) and basibranchials (bb) were absent in the TPH2 morphants. In the second arch, the ceratohyal cartilage was strongly reduced. Its size became shorter and appeared as a downward oriented line. The same orientation defect could be observed on the Merkel element in the first arch, the mandibular arch. There were no abnormalities neither in the development of the upper jaw, nor of the neurocranium of the TPH2 morphants.

TPH2 mRNA when injected with the morpholino, can rescue the TPH2 morphants phenotype indicating that craniofacial defects in the pharyngeal arches were specifically caused by blocking of TPH2 expression.

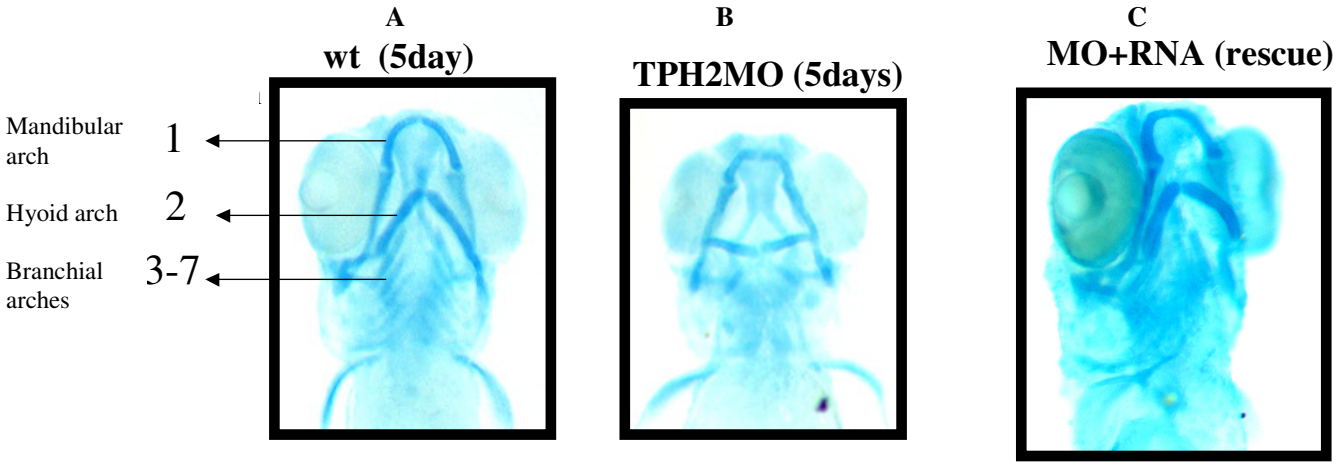

Fig. 3.22. Ventral view of pharyngeal arches of 5dpf embryos stained by alcian blue. Wild type (A), TPH2 morphants (B), and TPH2 morphants rescued by TPH mRNA (see text).

As mentioned above, 5HT single cells in the pharyngeal arches of 5 dpf TPH2 morphants were absent. We could not confirm, if those cells in the TPH2 morphants are still located in their normal position in the craniofacial tissue, but can not produce 5HT due to the inactivation of the TPH2 gene by the morpholino antisense, or if they are totally absent from the craniofacial tissue due the defects of the pharyngeal arches segmentation. For this confirmation we need to find another suitable specific antibody marker reacting with those cells.

To confirm the postulate that the defects in the pharyngeal arches of TPH2 knock down fish are - among other factors - caused by abnormalities in the neural crest cells development, and also to check if 5HT single cells are neural crest cell derivatives, we decided to knock down an earlier neural crest cell gene in the zebrafish, and then analyse the results. Recently it was reported, that Foxd3 morphants (Lister et al. 2006) show similar defects in the pharyngeal arches like TPH2 knock down fish. We used the same Foxd3 morpholino antisense sequence and injected one-cell zebrafish embryos. At 5 dpf, they showed a similar phenotype in the

pharyngeal arch like the TPH2 morphants, and moreover, they lack 5HT single cells located in the pharyngeal arches similar like TPH2 morphants (Fig. 3.23.).

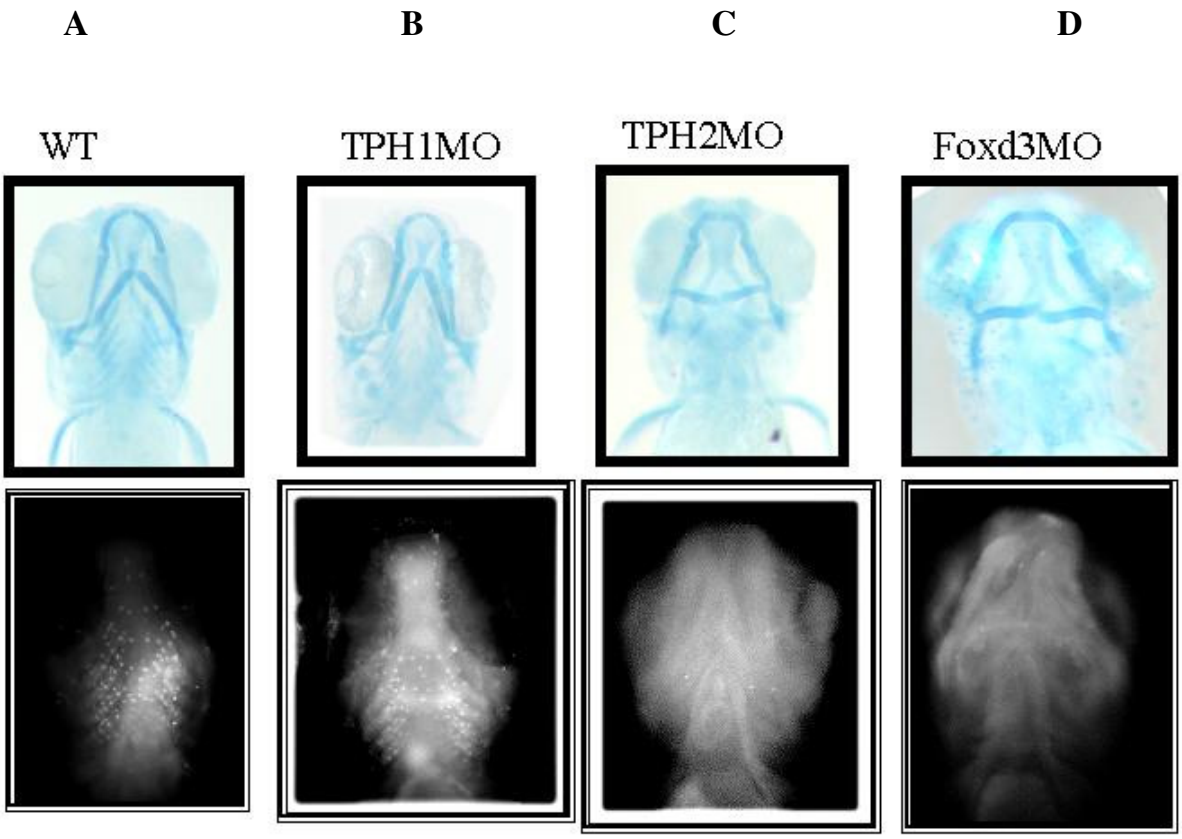

Fig. 3.23. Ventral view of pharyngeal arches of 5dpf of 4 groups, every group stained by alcian blue, and 5HT. Wild type (A), TPHD1 morphants (B), TPH2 morphants (C), and Foxd3 morphants (D) (see text).

3.4.2.2. Pigment cells

Zebrafish neural crest cells give rise to three types of pigmented cells: melanophores, xanthophores, and iridophores. The 2 days old TPH2 morphants exhibited reduction of the melanophores in comparison to the wild type (Fig. 3.24). Also the iridophores of the TPH2 morphants showed reduction particularly in the trunk and tail of the living larvae even on the 6th day (Fig. 3.25). The fish were photographed under incident light.

Fig. 3.24. Reduction of melanocytes in TPH2 morphants (TPH2MO) compared to wild type (WT) 2dpf fish embryos.

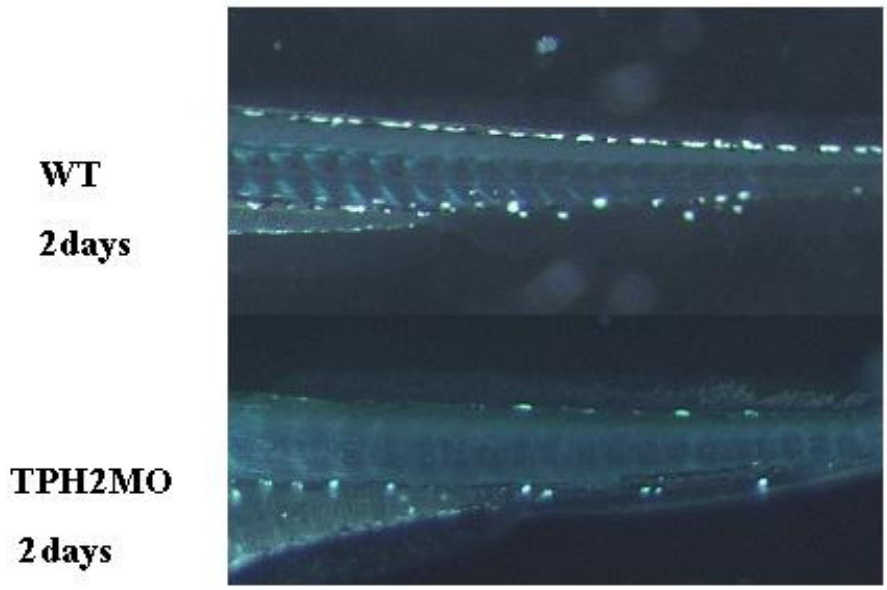

Fig. 3.25. Lateral view of 2dpf embryos shows reduction in iridophores of TPH2 morphants (TPH2MO) compared with wild type (WT).

3.4.2.3. Neural crest induction

To analyse the molecular mechanisms leading to the lack of some neural crest derivatives in the TPH2 knockdown fish, we examined if TPH2 affected the establishment of neural crest identity by analysing the expression of several early markers of neural crest cells by in situ hybridization or immunohistochemistry at different early developmental stages (5-, 10-, 15- , 20-somites). Protein biosynthesis and mRNA expression of Foxd3 and Sox9b respectively at the 5th-, and 10th-somite stage in the TPH2 morphants was similar like in the uninjected control embryos (Fig. 3.26). No significant differences could also be found in the expression of crestin, AP2α and snail2 between the controls and the TPH2 knockdown fishes at the 25th-somite stage.

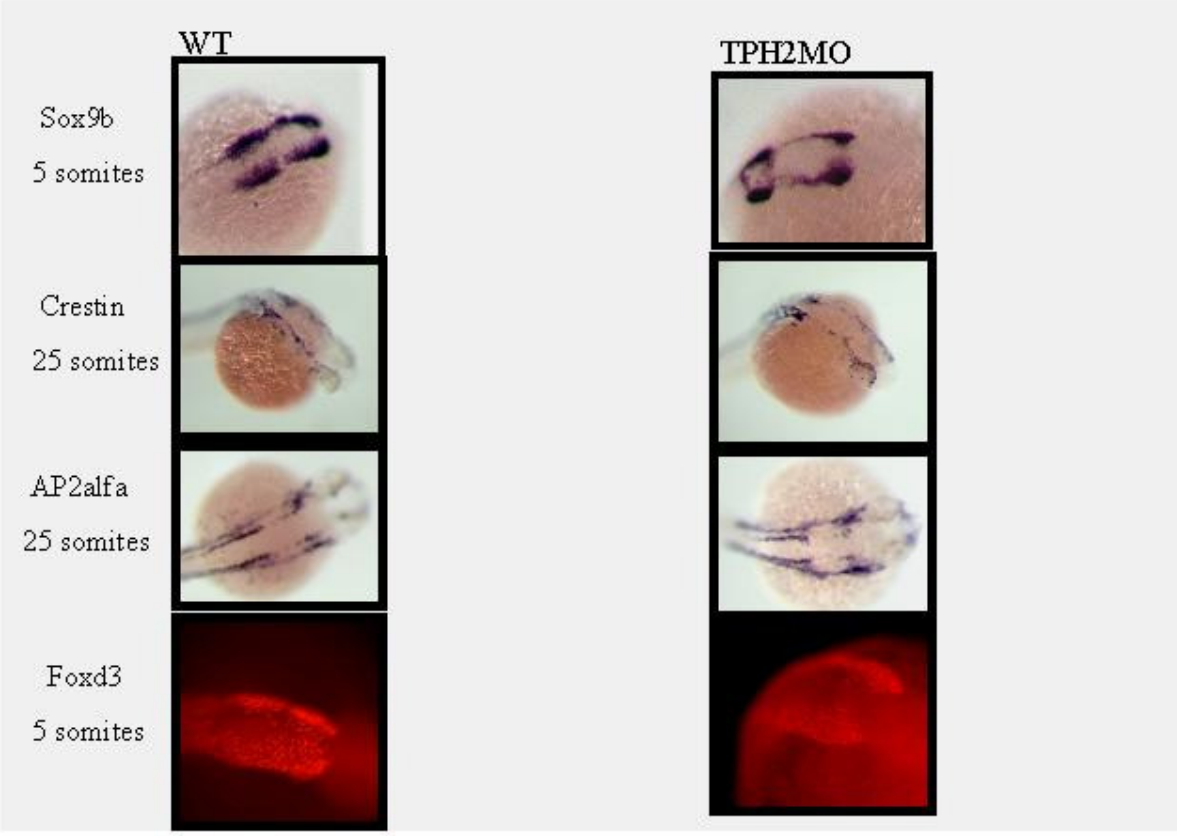

Fig. 3.26. Dorsal view of zebrafish embryos (left: wild type ˝WT˝ and right: TPH2 morphants ˝TPH2MO˝) at 5 somites and 25 somites showing by in situ hybridisation early neural crest markers Sox9b, Crestin, AP2α , and by immunostaining Foxd3. No differences in the expression of early neural crest cell markers in TPH2MO and WT embryos (see text).

3.4.2.4. Cranial neural crest cells migration

The cranial neural crest cells arise from the rhombomeres of the hindbrain, where TPH2 starts to be expressed. Three distinct streams migrate from rhombomeres (r) r1, r2 for the first stream, r4 for the second stream and r6 for the third stream of the hindbrain. These three streams migrate to the mandibular (1), the hyoid (2) and posterior (3) arches respectively. We utilized a riboprobe marker for the distal-less homo box 2 transcription factor, dlx2a, for in situ hybridization to follow the cranial crest migration during different stages (24-, 30-, 36-hpf), in TPH2 knockdown fish and controls. We could detect reduction of dlx2a expression in the three crest cell streams at 24 hpf stage and this reduction remained until the 30 hpf and 36 hpf stages in TPH2 morphants (Fig. 3.28). Afterwards, we analyzed the morphology of the hindbrain rhombomeres by in situ hybridization using a riboprobe for the transcription factor Pax2.1. A reduction in the expression of Pax2.1 in all rhombomeres of the hindbrain at the 24 hpf stage was observed in TPH2 morphants (Fig. 3.27).

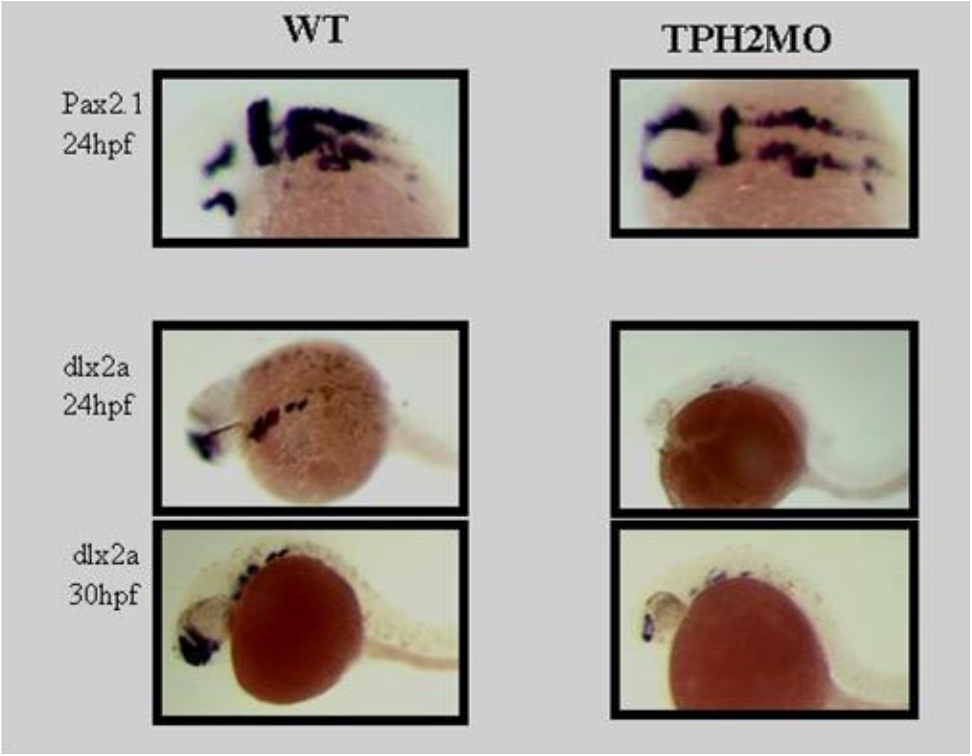

Fig. 3.27. Lateral view of zebrafish embryos (left: wild type ˝WT˝ and right: TPH2 morphants ˝TPH2MO˝) at 24hpf and 30hpf showing by in situ hybridisation Pax2.1 and Dlx2a. Fusion and reduction of migrating cranial neural crest cells (Dlx2a) may be due to hindbrain defects (Pax2.1) in TPH2MO in comparison to WT.

3.4.2.5. Myocardial function

After the ablation of the cardiac neural crest cells, chick embryos presented within hours myocardial dysfunction, suggesting a role for neural crest cells in myocardial maturation that is separate from its role in outflow septation. This role could be conserved in an animal that does not have a divided systemic and pulmonary circulation, such as the zebrafish (Li et al. 2003). To test this hypothesis, and according to the neural crest cell derivative phenotypes of our TPH2 zebrafish mutants, we observed defects in heart function starting from the 30 hpf stage. The heart tube failed to undergo looping, thus leading to a sharp decrease in the heart rate of up to 50% compared with the controls at the 36 hpf stage (Fig. 3.29.). Via a immunohistochemistry staining using the antibody MF20 (directed against myosin heavy chain, a specific cardiac muscle marker) we observed -contrary to controls- the absence of MF20 signals in the ventricular chamber.

To further analyse the role of serotonin in heart development, we inhibited the 5HT2B receptor by a pharmacological agent. This receptor is highly expressed in the heart of zebrafish embryos starting at 3 dpf (Fig. 3.34). Therefore, we incubated the embryos with different concentration of ritanserin, a specific 5HT2B blocker at 6 hpf. Twenty four hours afterwards, we could observe very slow blood circulation in the periphery, with a sharp decrease in the heart rate associated with oedema at a concentration of 10 μM. At 36 hpf the heart stopped to beat although the fish survived till 6 dpf.

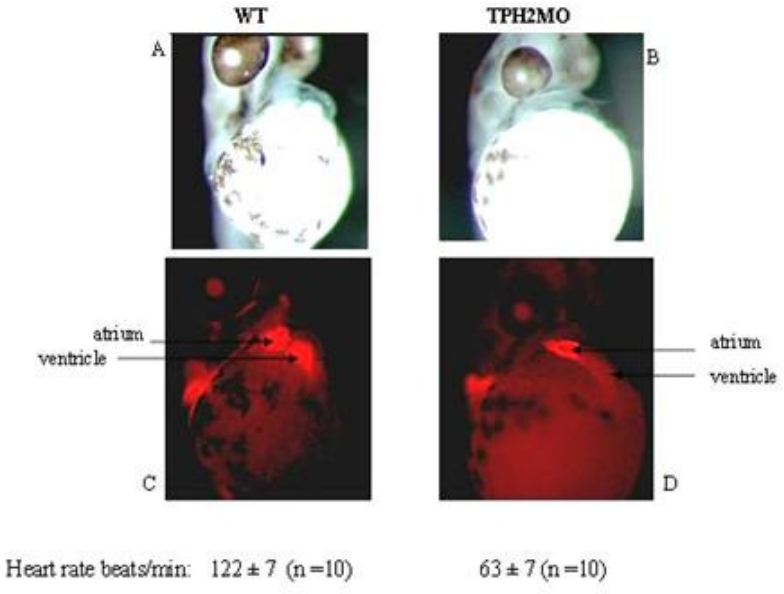

Fig. 3.28. 36hpf wild type (WT) (A and C), TPH2 morphants (TPH2MO) (B and D). Immunostaining with MF20 antibody to detect heart myosin. TPH2 morphants exhibit elongation in the heart tube, missing myosin from the heart ventricle, with reduction in heart rate in comparison to wild type (WT) (see text).

3.4.2.6. Peripheral nervous system

To identify the effect of TPH2 knockdown on the neural crest cell derivatives in the peripheral nervous system of the zebrafish, we stained the fish with a monoclonal antibody directed against the HNK1 carbohydrate at the 30 hpf stage. This molecule is expressed by Rohon-Beard and trigeminal ganglion neurons, both of which are primary sensory neurons that mediate touch sensitivity (Metcalfe et al. 1990) (Fig. 3.29).

The trigeminal sensory ganglion is located caudal to the developing eye, and the Rohon-Beard neurons are distributed along the spinal cord. The stained fibers on the head and rostral yolk sac are from the trigeminal neurons, while the fibers on the trunk and reminder of the yolk sac are from the Rohon-Beard neurons. McLean and Fetcho (2004) observed 5-HT reactivity in close proximity to the collaterals of the Rohon-Beard sensory neurons in spinal cord.

The trigeminal nerve of the TPH2 morphants was normally developed, but they lacked completely the Rohon-Beard neurons (Fig. 3.30). Probably due to this they lost the sensitivity for the touch response in the trunk part when being touched with a needle.

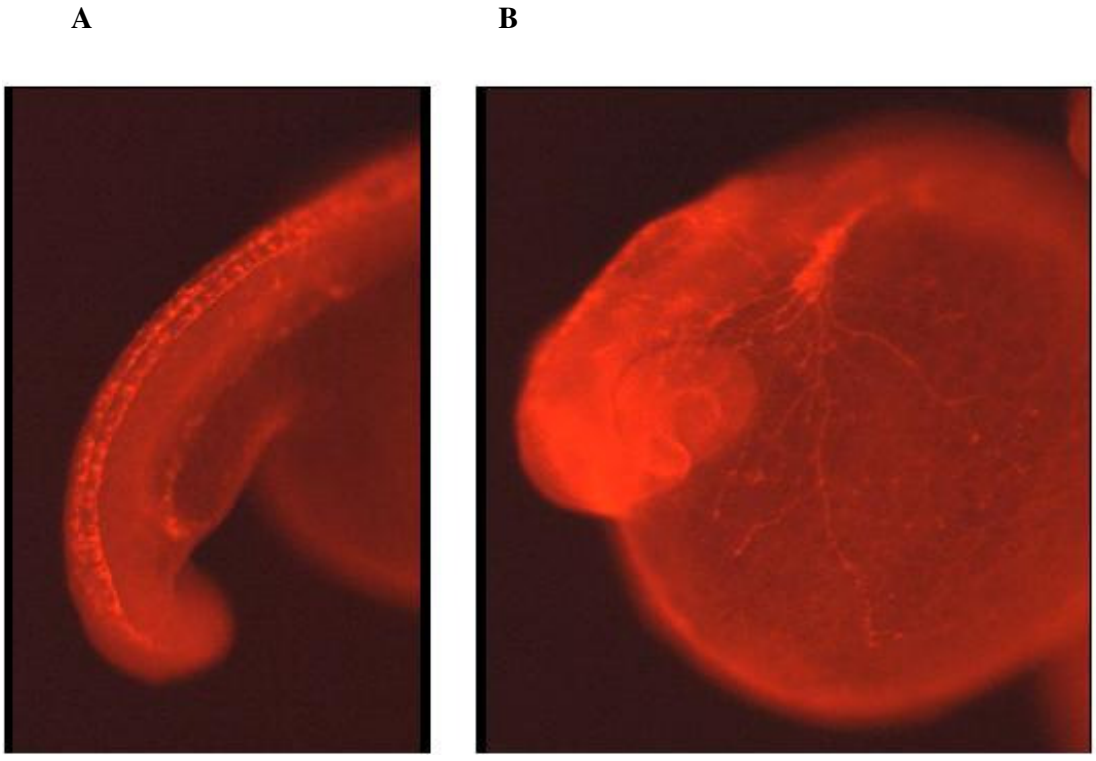

Fig. 3.29. Immunostaining with HNK1 antibody labelled primary neurons in dorsal trunk of 20 somites (A), and the trigeminal sensory neurons of 24 hpf (B) wild type embryos.

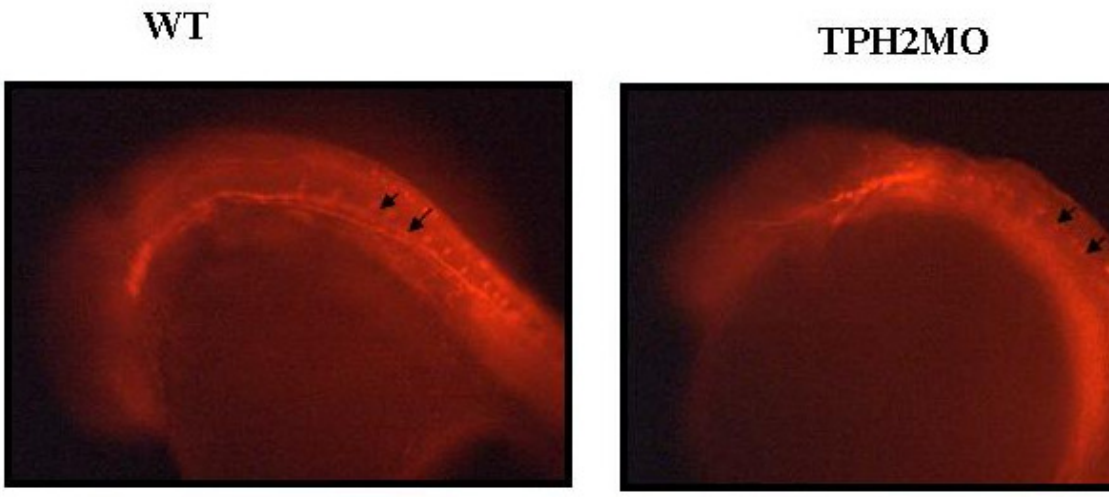

Fig. 3.30. Lateral view of 30hpf embryos stained with HNK1 antibody shows TPH2 morphants lack Rohon-Beard sensory neurons in spinal cord (arrow), while the trigeminal neurons developed normally like wild type embryos.

3.4.2.7. Motor neurons in the spinal cord region

Immunostaining using the ZN5 antibody detects cranial and spinal motor neurons in zebrafish embryos (Vanderlaan, et al. 2005). By means of a dorsal view of the hindbrain of 36 hpf old fish we could not see any difference in the cranial motor neurons located in the hindbrain boundaries of the wild type and TPH2 morphant fish. The motor neurons in the spinal cord region however, were missing in the TPH2 morphants in comparison to the wild type (Fig. 3.31).

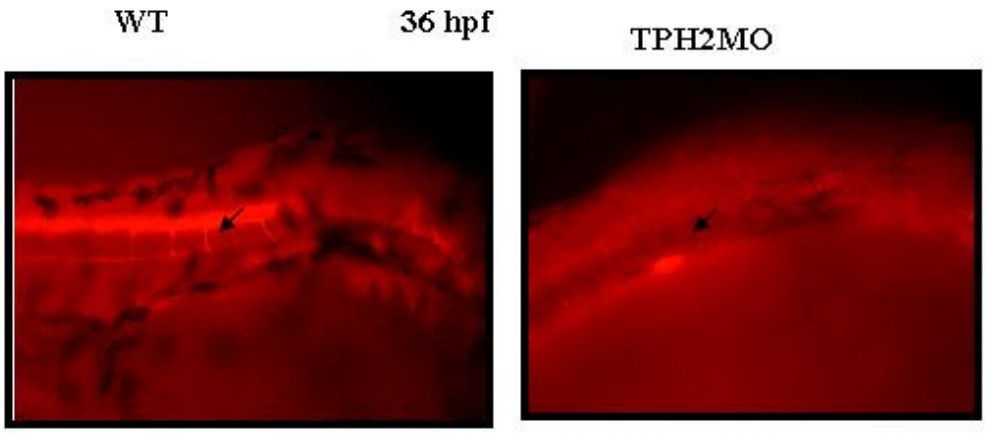

Fig. 3.31. Immunostaining using ZN5 antibody shows the absence of the motor neurons in the spinal cord region of 36hpf TPH2 morphants in comparison to wild type embryos.

3.4.2.8. Endodermal pharyngeal pouches

The formation of the endodermal pharyngeal pouches is the first indication of pharyngeal arch development (Veitch et al. 1999) and plays an important role in this process. These pouches pattern the neural crest cells along the anterior-posterior axis, and provide them with many signalling factors that they need in the pharyngeal arch development process. Many recent studies showed that defects in the endodermal pouches correlated with pharyngeal arch malformations like the zebrafish mutants *casanova*, and *van gogh*, which have defects in the endodermal pouches. These mutations showed also pharyngeal arch malformation, even though their neural crest cells were induced normally and migrated but were not correctly differentiated into the craniofacial elements and thus started to induce apoptosis, many of them in consequence died. Because of that we analysed by immunostaining using the antibody ZN5 (that could detect the endodermal pouches in 30 hpf old zebrafish larvae, and in the wild type fish), the pouches of TPH2 morphants. The endodermal pouch segments turned out to be missing (Fig. 3.32).

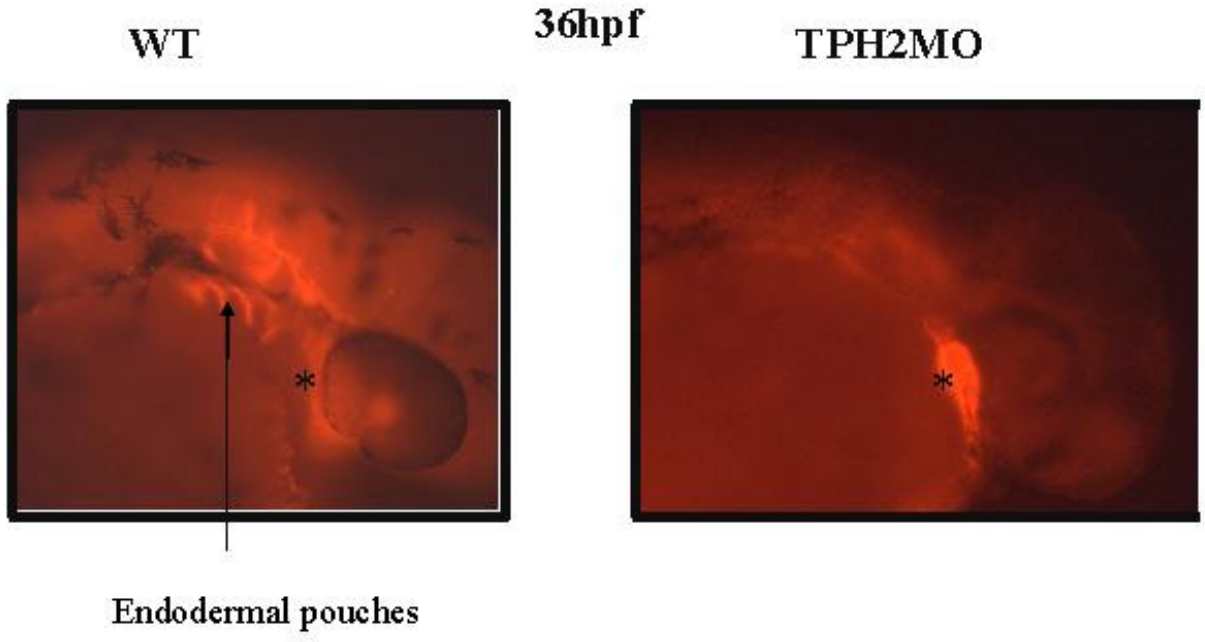

Fig. 3.32. Immunostaining with ZN5 antibody of 36hpf embryos shows absence of endodermal pouches in TPH2 morphants in comparison to wild type (arrow), while the elongated heart of the morphants still giving ZN5 positive signal like the normal heart of the wild type*.

3.5. 5HT2B receptor in zebrafish

To study the developmental role of 5HT in craniofacial morphogenesis, we investigated which candidate 5HT receptor or receptors are involved in this process. The mouse 5HT2B receptor has been shown to participate in craniofacial and cardiac morphogenetic events (Shuey et al. 1993, Yavarone et al. 1993, Choi et al. 1997). It was observed that 5HT2B is expressed in mouse embryos with a peak of expression at E 8.5. By whole mount in situ hybridisation and immunohistochemistry 5HT2B expression has been detected in neural crest cells, myocardium, and in the pharyngeal arches. Therefore we studied the expression pattern of this receptor and its function in zebrafish.

3.5.1. Cloning of the 5HT2B receptor

We screened the zebrafish genome bank using mammalian 5HT2B sequences. By this way we could clone the full length cDNA of 5HT2B receptor of zebrafish and submitted it to GenBank (DQ864496).

The 5HT2B receptor gene is located on chromosome 22, and contains 3 exons and 2 introns like all other vertebrate 5HT2B receptors genes (Fig. 3.34).

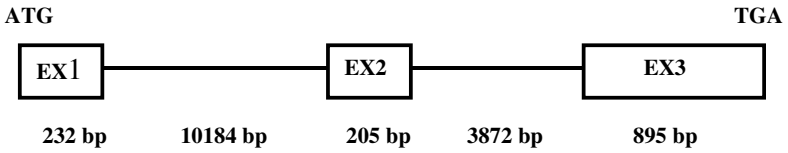

Fig. 3.34. Structure of the zebrafish 5HT2B receptor gene

When the zebrafish 5HT2B receptor amino acid sequence was compared with known sequences from tetraodon, xenopus, human, macaca, rat and mouse an amino acid identity was detected of 65%, 60%, 60%, 58%, 58% and 56%, respectively (Table 2). The homology is even higher in the transmembrane regions. The N-terminal domain is shorter and not homologous to mammalian receptors, but of similar length if compared to tetraodon and xenopus. The zebrafish 5HT2B amino acid sequence is closely related to that of tetraodon, especially because of some amino acid insertions in the fourth transmembrane domain and in the fifth extracellular loop (Fig. 3.35, 3.36).

SeqA	Name	Len(aa)	SeqB	Name	Len(aa)	Score
1	Tetraodon	471	2	Danio	443	65
1	Tetraodon	471	3	Xenopus	453	56
1	Tetraodon	471	4	human	481	54
1	Tetraodon	471	5	Mus	479	50

1	Tetraodon	471	6	Rattus	479	50
1	Tetraodon	471	7	Macaca	460	55
2	Danio	443	3	Xenopus	453	60
2	Danio	443	4	human	481	60
2	Danio	443	5	Mus	479	56
2	Danio	443	6	Rattus	479	58
2	Danio	443	7	Macaca	460	58
3	Xenopus	453	4	human	481	65
3	Xenopus	453	5	Mus	479	60
3	Xenopus	453	6	Rattus	479	60
3	Xenopus	453	7	Macaca	460	62
4	human	481	5	Mus	479	82
4	human	481	6	Rattus	479	80
4	human	481	7	Macaca	460	98
5	Mus	479	6	Rattus	479	89
5	Mus	479	7	Macaca	460	80
6	Rattus	479	7	Macaca	460	78

Table 2. Comparison of amino acid sequences of 5HT2B receptor from different species (see text)

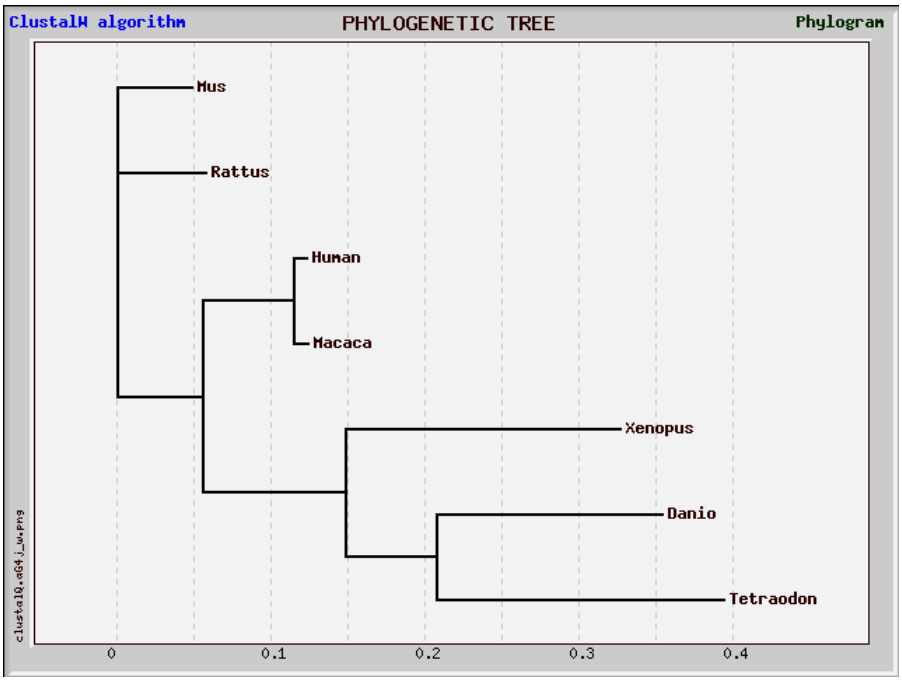

Fig. 3.35. Phylogenetic tree of 5HT2B receptors from different species. 5HT2B receptor amino acid sequence of zebrafish is more similar to the sequences of tetraodon and xenopus more than mammals.

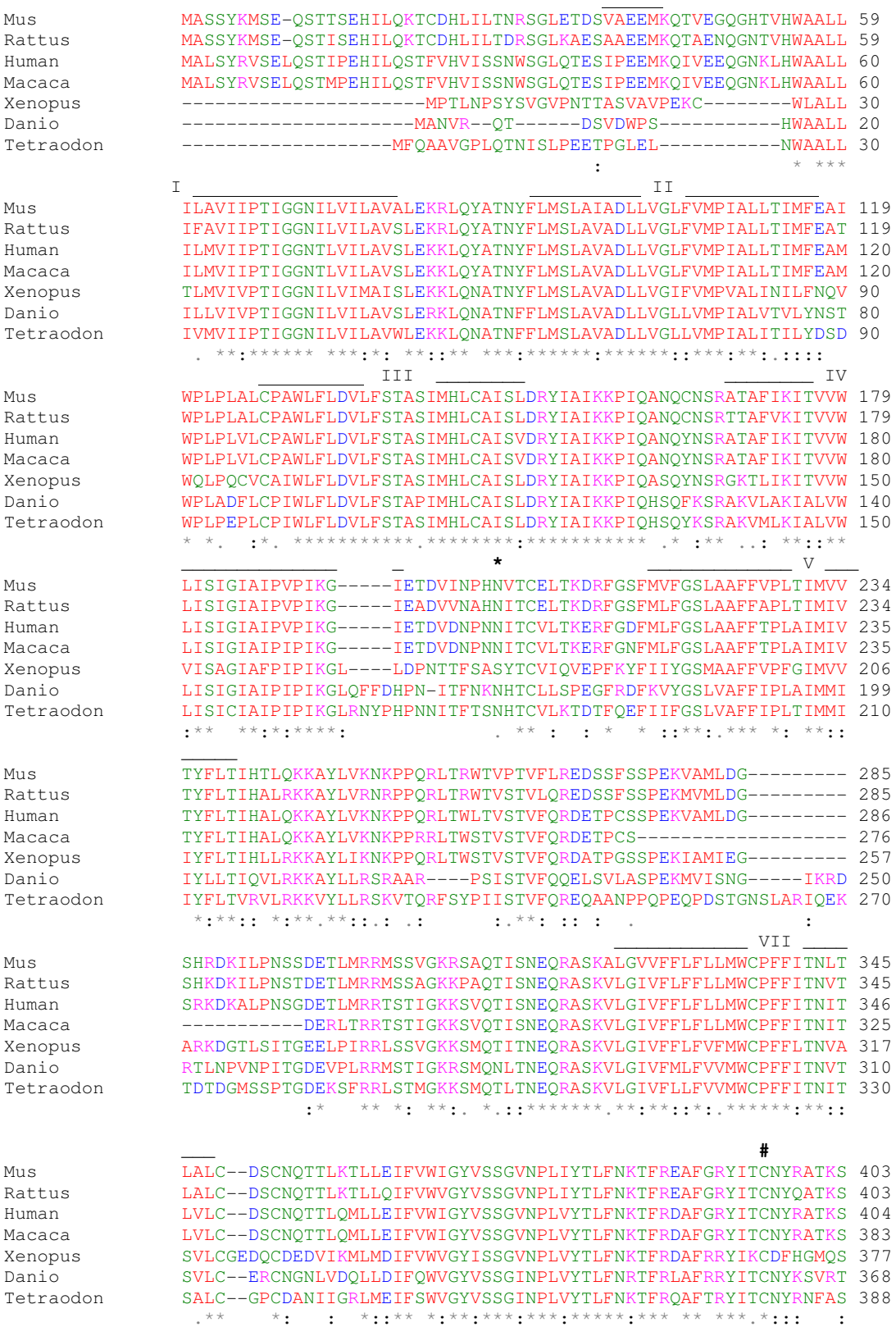
Mus MASSYKMSE-QSTTSEHILQKTCDHLILTNRSGLETDSVAEEMKQTVEGQGHTVHWAALL 59
Rattus MASSYKMSE-QSTISEHILQKTCDHLILTDRSGLKAESAAEEMKQTAENQGNTVHWAALL 59
Human MALSYRVSELQSTIPEHILQSTFVHVISSNWSGLQTESIPEEMKQIVEEQGNKLHWAALL 60
Macaca MALSYRVSELQSTMPEHILQSTFVHVISSNWSGLQTESIPEEMKQIVEEQGNKLHWAALL 60
Xenopus ----------MPTLNPSYSVGVPNTTASVAVPEKC--------WLALL 30
Danio ----------MANVR--QT------DSVDWPS-----------HWAALL 20
Tetraodon ----------MFQAAVGPLQTNISLPEETPGLEL-----------NWAALL 30
I II
Mus ILAVIIPTIGGNILVILAVALEKRLQYATNYFLMSLAIADLLVGLFVMPIALLTIMFEAI 119
Rattus IFAVIIPTIGGNILVILAVSLEKRLQYATNYFLMSLAVADLLVGLFVMPIALLTIMFEAT 119
Human ILMVIIPTIGGNTLVILAVSLEKKLQYATNYFLMSLAVADLLVGLFVMPIALLTIMFEAM 120
Macaca ILMVIIPTIGGNTLVILAVSLEKKLQYATNYFLMSLAVADLLVGLFVMPIALLTIMFEAM 120
Xenopus TLMVIVPTIGGNILVIMAISLEKKLQNATNYFLMSLAVADLLVGIFVMPVALINILFNQV 90
Danio ILLVIVPTIGGNILVILAVSLERKLQNATNFFLMSLAVADLLVGLLVMPIALVTVLYNST 80
Tetraodon IVMVIIPTIGGNILVILAVWLEKKLQNATNFFLMSLAVADLLVGLLVMPIALITILYDSD 90
III IV
Mus WPLPLALCPAWLFLDVLFSTASIMHLCAISLDRYIAIKKPIQANQCNSRATAFIKITVVW 179
Rattus WPLPLALCPAWLFLDVLFSTASIMHLCAISLDRYIAIKKPIQANQCNSRTTAFVKITVVW 179
Human WPLPLVLCPAWLFLDVLFSTASIMHLCAISVDRYIAIKKPIQANQYNSRATAFIKITVVW 180
Macaca WPLPLVLCPAWLFLDVLFSTASIMHLCAISVDRYIAIKKPIQANQYNSRATAFIKITVVW 180
Xenopus WQLPQCVCAIWLFLDVLFSTASIMHLCAISLDRYIAIKKPIQASQYNSRGKTLIKITVVW 150
Danio WPLADFLCPIWLFLDVLFSTAPIMHLCAISLDRYIAIKKPIQHSQFKSRAKVLAKIALVW 140
Tetraodon WPLPEPLCPIWLFLDVLFSTASIMHLCAISLDRYIAIKKPIQHSQYKSRAKVMLKIALVW 150
V
Mus LISIGIAIPVPIKG-----IETDVINPHNVTCELTKDRFGSFMVFGSLAAFFVPLTIMVV 234
Rattus LISIGIAIPVPIKG-----IEADVVNAHNITCELTKDRFGSFMLFGSLAAFFAPLTIMIV 234
Human LISIGIAIPVPIKG-----IETDVDNPNNITCVLTKERFGDFMLFGSLAAFFTPLAIMIV 235
Macaca LISIGIAIPIPIKG-----IETDVDNPNNITCVLTKERFGNFMLFGSLAAFFTPLAIMIV 235
Xenopus VISAGIAFPIPIKGL----LDPNTTFSASYTCVIQVEPFKYFIIYGSMAAFFVPFGIMVV 206
Danio LISIGIAIPIPIKGLQFFDHPN-ITFNKNHTCLLSPEGFRDFKVYGSLVAFFIPLAIMMI 199
Tetraodon LISICIAIPIPIKGLRNYPHPNNITFTSNHTCVLKTDTFQEFIIFGSLVAFFIPLTIMMI 210
VII
Mus TYFLTIHTLQKKAYLVKNKPPQRLTRWTVPTVFLREDSSFSSPEKVAMLDG--------- 285
Rattus TYFLTIHALRKKAYLVRNRPPQRLTRWTVSTVLQREDSSFSSPEKMVMLDG--------- 285
Human TYFLTIHALQKKAYLVKNKPPQRLTWLTVSTVFQRDETPCSSPEKVAMLDG--------- 286
Macaca TYFLTIHALQKKAYLVKNKPPRRLTWSTVSTVFQRDETPCS------------------- 276
Xenopus IYFLTIHLLRKKAYLIKNKPPQRLTWSTVSTVFQRDATPGSSPEKIAMIEG--------- 257
Danio IYLLTIQVLRKKAYLLRSRAAR----PSISTVFQQELSVLASPEKMVISNG-----IKRD 250
Tetraodon IYFLTVRVLRKKVYLLRSKVTQRFSYPIISTVFQREQAANPPQPEQPDSTGNSLARIQEK 270
#
Mus SHRDKILPNSSDETLMRRMSSVGKRSAQTISNEQRASKALGVVFFLFLLMWCPFFITNLT 345
Rattus SHKDKILPNSTDETLMRRMSSAGKKPAQTISNEQRASKVLGIVFLFFLLMWCPFFITNVT 345
Human SRKDKALPNSGDETLMRRTSTIGKKSVQTISNEQRASKVLGIVFFLFLLMWCPFFITNIT 346
Macaca -----------DERLTRRTSTIGKKSVQTISNEQRASKVLGIVFFLFLLMWCPFFITNIT 325
Xenopus ARKDGTLSITGEELPIRRLSSVGKKSMQTITNEQRASKVLGIVFFLFVFMWCPFFLTNVA 317
Danio RTLNPVNPITGDEVPLRRMSTIGKRSMQNLTNEQRASKVLGIVFMLFVVMWCPFFITNVT 310
Tetraodon TDTDGMSSPTGDEKSFRRLSTMGKKSMQTLTNEQRASKVLGIVFLLFVVMWCPFFITNIT 330
Mus LALC--DSCNQTTLKTLLEIFVWIGYVSSGVNPLIYTLFNKTFREAFGRYITCNYRATKS 403
Rattus LALC--DSCNQTTLKTLLQIFVWVGYVSSGVNPLIYTLFNKTFREAFGRYITCNYQATKS 403
Human LVLC--DSCNQTTLQMLLEIFVWIGYVSSGVNPLVYTLFNKTFRDAFGRYITCNYRATKS 404
Macaca LVLC--DSCNQTTLQMLLEIFVWIGYVSSGVNPLVYTLFNKTFRDAFGRYITCNYRATKS 383
Xenopus SVLCGEDQCDEDVIKMLMDIFVWVGYISSGVNPLVYTLFNKTFRDAFRRYIKCDFHGMQS 377
Danio SVLC--ERCNGNLVDQLLDIFQWVGYVSSGINPLVYTLFNRTFRLAFRRYITCNYKSVRT 368
Tetraodon SALC--GPCDANIIGRLMEIFSWVGYVSSGINPLVYTLFNKTFRQAFTRYITCNYRNFAS 388

```
Mus             VKALR--------KFSSTLCFGNSMVENSKFFTKHGIRNGINPAMYQSPMRLRSSTIQSS 455
Rattus          VKVLR--------KCSSTLYFGNSMVENSKFFTKHGIRNGINPAMYQSPVRLRSSTIQSS 455
Human           VKTLR--------KRSSKIYFRNPMAENSKFFKKHGIRNGINPAMYQSPMRLRSSTIQSS 456
Macaca          VKTLR--------KRSSKIYFRNPTAENSKFFKKHGIRNGINPAMYQSPMRLRSSTIQSS 435
Xenopus         VKLLR--------NCSSRISFRNSMAENSKLIMKHGMKNGINPVMYQSPLRLCNAQLESS 429
Danio           PKLQR----------RSKISFRSSVTENSKRFMKHGMKNGISPVGYQSPIRHRSTQLQTS 418
Tetraodon       KEQGRSFRASTVDRMLTHISPRSSVAENAKLFTKQEIKN--ETTDYRSPLGCLQPSAQTS 446
                 :  *           : :   .. .**:* : *: ::* :... *:**:   ..  ::*

Mus             SIILLDT-LLTENDGDKAEEQVSYI 479
Rattus          SIILLNT-FLTENDGDKVEDQVSYI 479
Human           SIILLDTLLLTENEGDKTEERVSYV 481
Macaca          SIILLDTLLLTENEGDKTEEQVSYV 460
Xenopus         -AILLDTLLLTENEAGKTEEQASYV 453
Danio           ANIMLDTLLLTDNEDCKPDEHVSHV 443
Tetraodon       TGVVLDKILLTHTENCKQEERVSCV 471
                  ::*:.::**..:  * :::.* :
```

Fig. 3. 36. Alignment of amino acid sequences of zebrafish 5HT2B with homologous vertebrate 5HT2Bs. The seven transmembrane domains are indicated by lines above the sequence and labeled with Roman numerals. An asterisk indicates the conserved N-glycosylation site in the second extracellular loop and a square denotes the position of the presumptive palmitoylation acceptor site at a conserved cysteine residue in the carboxyl terminus.

3.5.2. Expression pattern of 5HT2B receptor in zebrafish embryos

Based on the cloned zebrafish 5HT2B full length cDNA, we prepared a riboprobe and determined the expression of this receptor by in situ hybridisation. Its expression was restricted to the heart and pharyngeal arches. Expression started first in 2 dpf embryos and persisted at least until the fish were 4 days old. We could not detect 5HT2B expression in the neural crest cells at least not during their induction or migration.

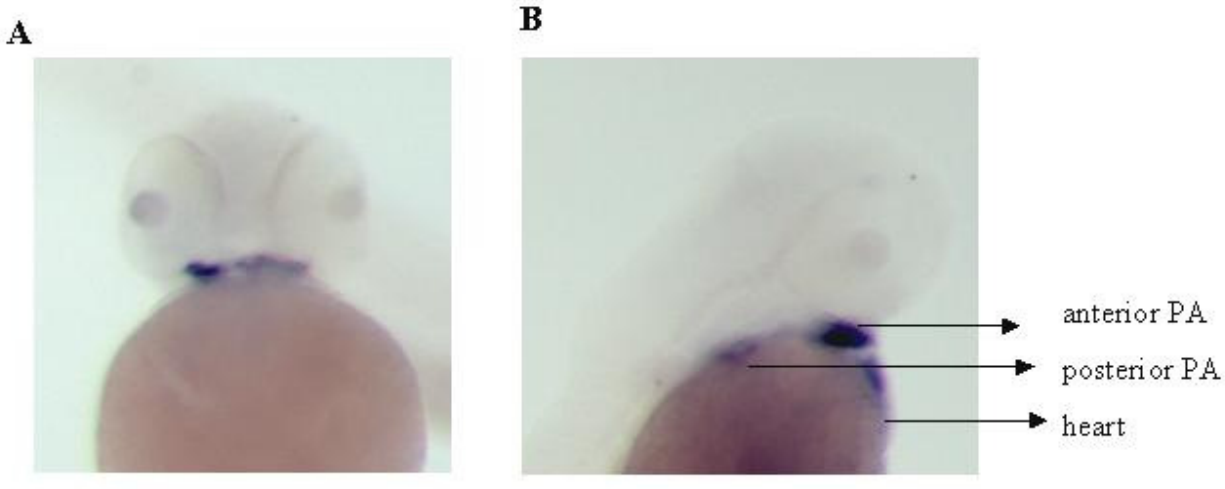

Fig. 3.34. In situ hybridization of 3 dpf of zebrafish embryos with a 5HT2B riboprobe. (A) ventral view (B) lateral view. The 5HT2B receptors expressed in different pharyngeal arches and in heart.

2.5.3. Loss-of function test of 5HT2B receptor

We used two methods to block the 5HT2B receptor: the first method was pharmacological, the second genetic.

2.5.3.1. Pharmacological loss-of function test

Many studies showed that, ritanserin is a specific antagonist of 5HT2 receptors, with highest specifity for the 5HT2B receptor (Buznikov 2005). We exposed fish embryos starting from the blastula stage (4hpf) to different concentrations of ritanserin (5, 10 and 20 μM) disolved in the fish water for 5 days. By using alcian blue staining we detected slight craniofacial malformations (Fig. 3.38), comparable but less pronounced than in the TPH2 morphants. The defects were restricted to the mandibular and hyoid arches. Their structures were smaller in size and were misshaped. Furthermore, they were oriented more downward in comparison to the posterior branchial arches, that were not affected by ritanserin. In the wild type all the pharyngeal arches of the lower jaw were located in the same level.

When fish embryos were treated from the first minutes after fertilization with ritanserin with the same concentrations, the embryos died before they reached the gastrula stage.

To follow the temporal effect of ritanserin in pharyngeal arches development, we divided fish embryos in five groups, and every group was treated with ritanserin only for one day:

the first group treated with ritanserin only during the first day, the second group treated with ritanserin only during the second day etc…At the end of the fifth day all the groups were fixed and stained with alcian blue. Ritanserin had no effect on the pharyngeal arches development of the first and the second group. Embryos in the third, fourth and fifth group exhibited the same defects in the pharyngeal arches as observed, when ritanserin was exposed to the fish during all 5 days (data not shown).

2.5.3.2. Genetic loss-of-function test

We injected one-cell embryo with morpholino antisense oligonucleotides against the 5HT2B receptor and stained the fishes with alcian blue at 5dpf. We observed that 5HT2B morphants exhibited similar defects in the pharyngeal arches like ritanserin treated embryos (Fig. 3.38).

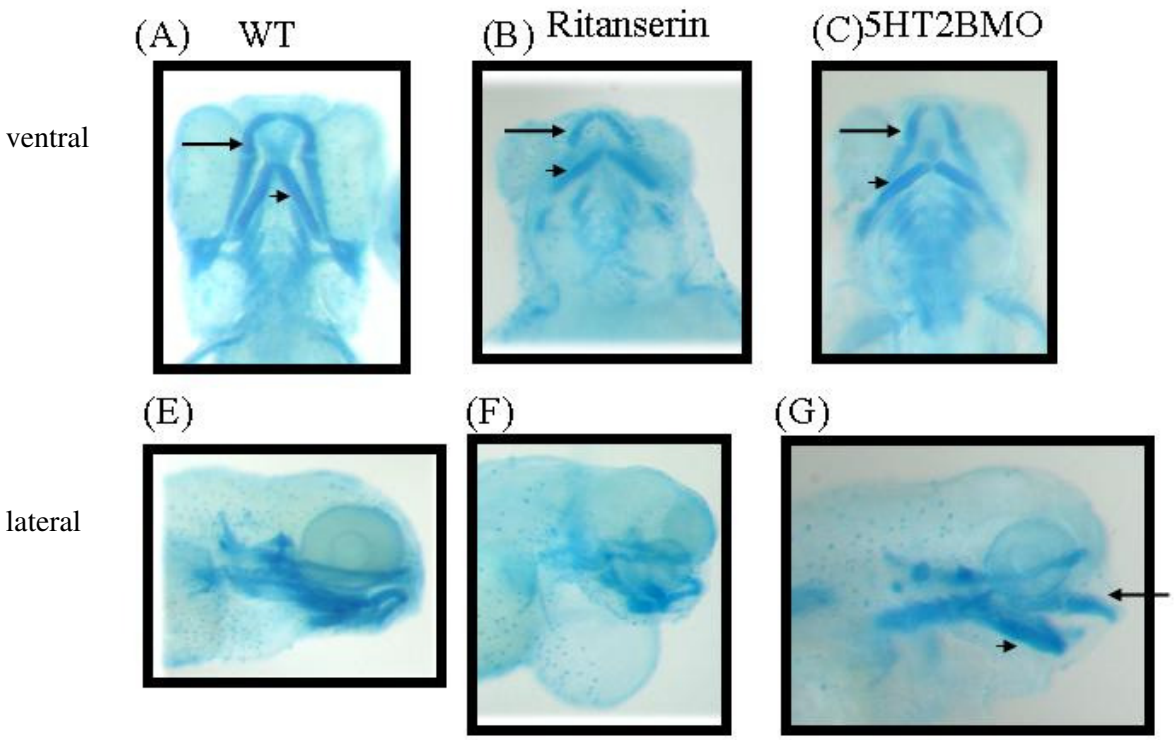

Fig. 3.38 Alcian blue staining of pharyngeal arches of 5dpf zebrafish embryos. (A,B,C) ventral view; (E,F,G) lateral view. (A ,E) wild type; (B,F) treated with ritanserin; (C,G) 5HT2B morphants. The mandibular (arrow) and hyoid (arrow head) arches of ritanserin treated embryos and 5HT2B morphants were oriented downwards in comparison to the wild type (WT).

3.6. Cloning of tryptophan hydroxylase of Drosophila melanogaster

The identification of only one gene, Henna, encoding both tryptophan hydroxylase and phenylalanine hydroxylase (PAH) activity in Drosophila melanogaster (Neckameyer and White 1992) led to the hypothesis, that in drosophila as well as in other insects, only two aromatic amino acid hydroxylases (AAAH) exist, tyrosine hydroxylase, and one other enzyme (termed Henna) for the hydroxylation of both phenylalanine (Phe) and tryptophan (Trp) (Alcaniz et al. 1997).

Nevertheless, we searched in the drosophila genome project, and we could identify an additional gene (CG9122) which encodes a cDNA, whose translated protein sequence was highly homologous to mammalian tryptophan hydroxylase. In fact, the homology of this sequence to mammalian TPH was even higher than that of Henna. The Gene CG9122 located in chromosome 3, the DNA genome contains around 2780 bp, and the full length of coding cDNA contains 1716 bp, the whole gene contains 7 exons, and 6 introns.

To compare the hydroxylation of Trp and Phe by Henna and the CG9122 gene product (we termed it DmTPH), we cloned the full length of cDNA of both enzymes in the expression vector pcDNA 3.1 and transfected this vectors into COS7 cells. We then used two different methods to compare their ability to hydroxylate tryptophan.

First, we measured the enzyme activity of tryptophan hydroxylase using HPLC. By this method we can determine which enzyme can hydroxylate tryptophan better than the other and quantify the amount of product (hydroxylated tryptophan). We compared the phenylalanine hydroxylase activity of both enzymes by a colorimetric assay. As positive control sample for TPH activity we used mouse intestine tissue, as positive control sample for PAH activity we used mouse liver tissue. (Fig. 3.39) shows that DmTPH can hydroxylate Trp more than 3 times faster than Henna. The differences between DmTPH and Henna were more clear when we determined the enzyme kinetic parameters Vmax and the Km value for Trp (Table 3).

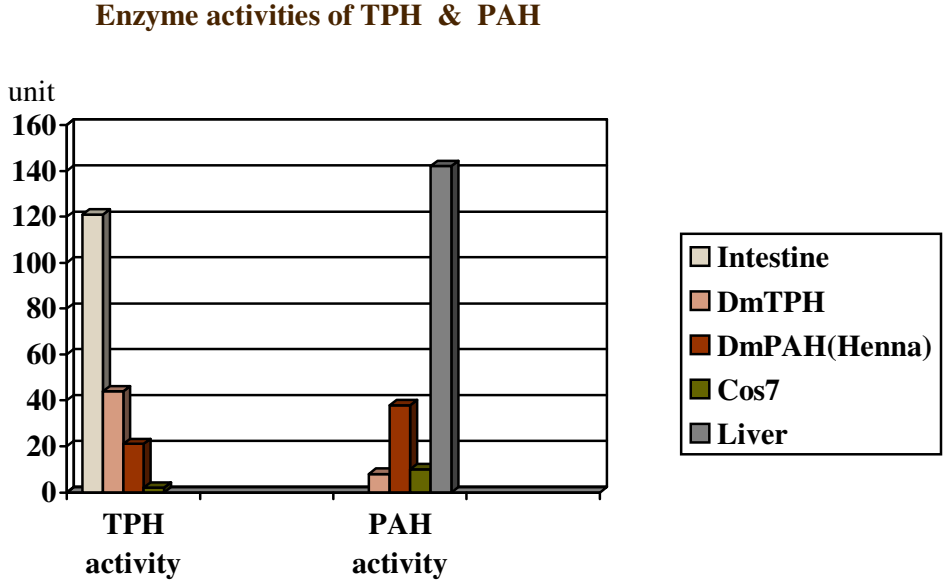

Fig. 3.39. COS7 cells transfected with DmTPH can hydroxylate tryptophan more than COS7 cells transfected with DmHenna, while they have no PAH activity on the opposite of COS7 cells transfected with Henna, that can hydroxylate phenylalanine. Intestine tissues was positive control for TPH activity, liver tissues was positive control for PAH activity, and non-transfected COS7 cells were used as blank.

	DmTPH	Henna
Vmax	86.6	37.5
Km	36.8	210.3

Table 3. Comparison between DmTPH and Henna for the Vmax and Km value for tryptophan.

The second method we used to compare DmTPH and Henna was the effect of 7-hydroxytryptophan (7-OHTrp) on DmTPH expressing COS7 cells and Henna expressing COS7 cells. It is known that TPH metabolizes 7-OHTrp to the toxin 5,7-Dihydroytryptophan (5,7-DHT), which is metabolized to radical anions and H_2O_2 and that thereby induces cellular suicide by apoptosis (Walther et al. 2002). Therefore 7-OHTrp is toxic only for TPH expressing cells.

Fig. 3.40 shows that 7-OHTrp has no toxic effect at concentrations of 5 mM or 10 mM on control COS7 cells. When those cells expressed Henna (PAH), 20% of the cells died after 24h when incubated with 5 mM 7-OHTrp. This percentage increased to 40% when the concentration of 7-OHTrp was increased to 10 mM (Fig. 3.40 B). However 7-OHTrp was highly toxic to COS7 cells expressing DmTPH. More than 50% of the cells started to die after 1 day of exposure to 5 mM 7-OHTrp. When the concentration was increased to 10 mM only

less than 30% of DmTPH expressing COS7 survived (Fig. 3.40 C). The results of these experiments show that the apoptosis rate of the cells correlates with their ability to hydroxylate 7-OHTrp producing the toxic product 5,7-DHT. This effect was stronger in DmTPH expressing COS7 cells than in the henna expressing COS7 cells. To confirm this observation and to show that this toxic effect of 7-OHTrp is only due its hydroxylation by TPH and PAH, we tested whether the inhibition of this enzyme was able to protect the cells against the toxicity of 7-OHTrp. We thus used pCPA, a highly specific, and irreversible inhibitor for both TPH and PAH. As shown in (Fig. 3.41 A) there is no toxic effect on the control COS7 cells, and when they were treated with 10 mM 7-OHTrp, 5 mM pCPA or both together. When they expressed Henna, the toxic effect of 7-OHTrp could be protected by pCPA (Fig. 3.41 B). This protection against the toxicity was more pronounced in DmTPH expressing COS7 cells (Fig. 3.41C). These results are confirming that the toxicity of 7-OHTrp is only due its hydroxylation in C5 to produce the toxic compound 5,7-DHT. This toxicity was again correlated with the rate of the hydroxylation of 7-OHTrp by the transfected enzyme DmTPH or henna (PAH), which is obviously higher for DmTPH.

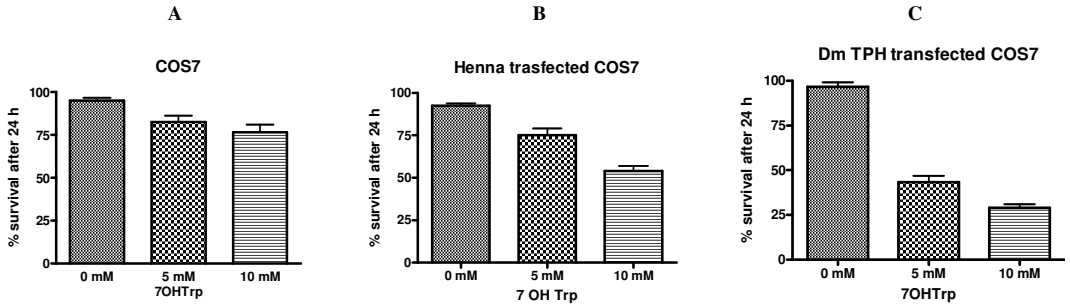

Fig. 3.40. The toxicity of 7-OHTrp for COS7 cells is higher when they express DmTPH than when they express Henna (see text).

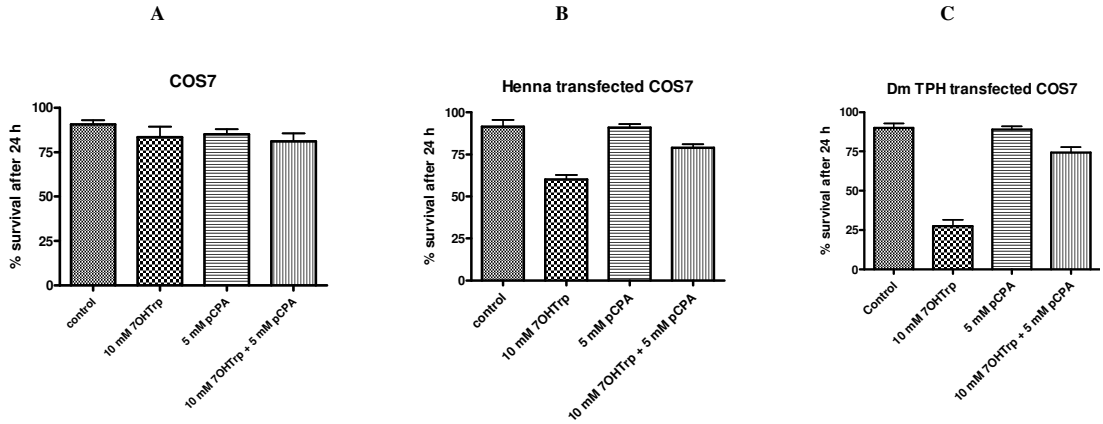

Fig. 3.41. PCPA can protect the cells against the toxicity of 7-OHTrp (see text).

3.7. Knock out of TPH2 in the mouse

In order to generate mice that lack TPH2, we designed a targeting construct in the pTV0 vector, in which the translated portion of the fifth coding exon and the proximal part of the following intron of the TPH2 gene were substituted with a neomycin-resistance selection cassette (Fig. 3.42) and two arms for homologous recombination (short arm with around 1 kb before the neomycin cassette and long arm with around 7 kb behind it).

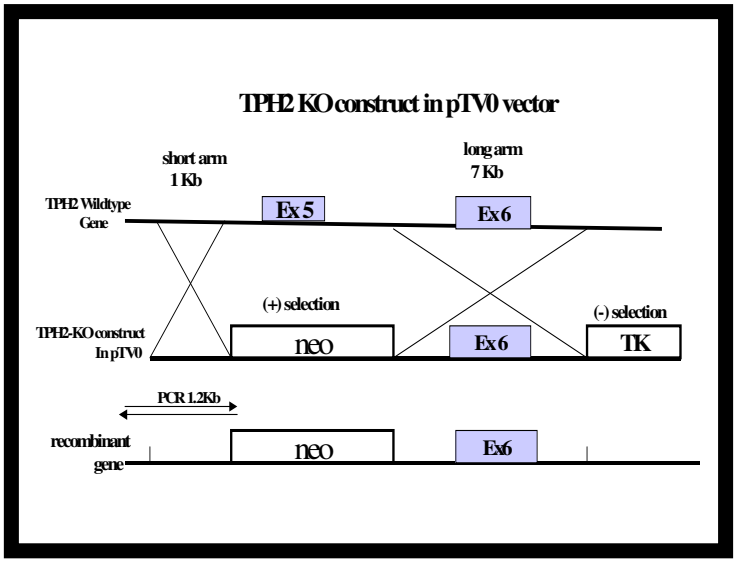

Fig. 3.42. TPH2 targeting construct: Exon 5 (Ex5) in the TPH2 gene will be replaced by homologous recombination with the neomycin cassette (see text).

The TPH2 targeting construct was linearized at the single *ClaI* site. After several rounds of electroporation into the ES cells more than 1000 ES clones were picked. To test for the correct integration of the targeting construct in the ES cells genome, we designed a reverse primer in the neomycin cassette, and a forward primer before the short arm in a PCR. We could amplify a 1.2 Kb band from the DNA of the single positive ES clone that we found (Fig.3.41). By injecting more than 400 blastocysts with positive ES cells, and then transplanting them to foster mothers as shown in Fig. 3.43, we obtained 12 chimeras, 6 males and 6 females. However all chimeras when bred with C57Bl/6 mice gave birth only to C57Bl/6 mice, but not to ES cell derived offspring.

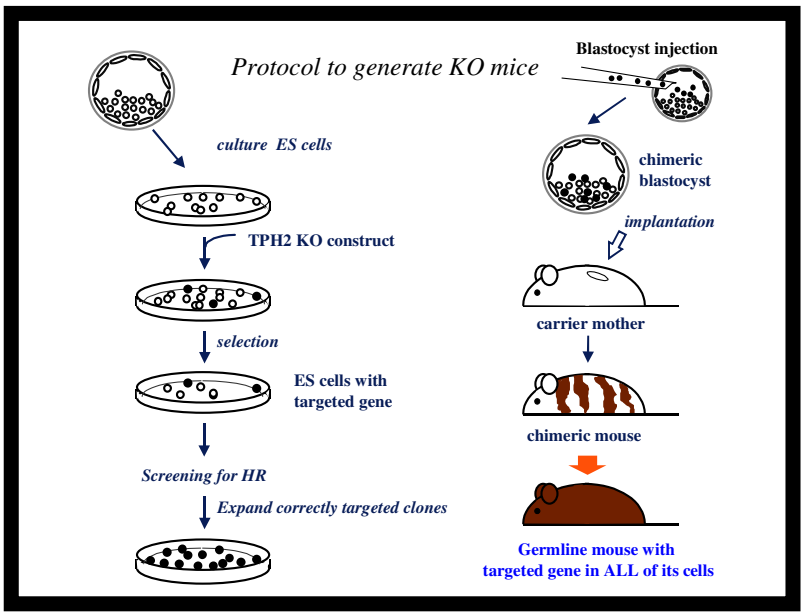

Fig. 3.43. The steps of the standard protocol to generate knockout mice.

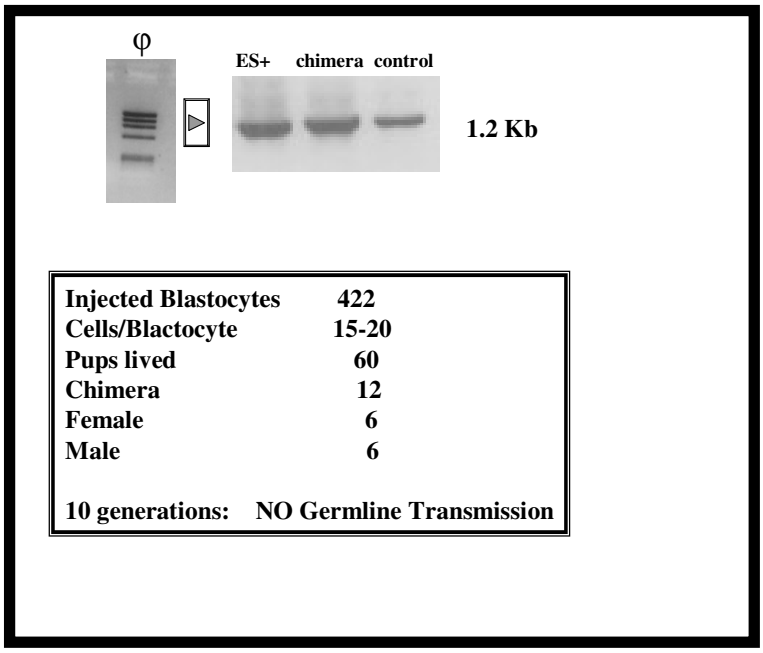

Fig. 3.44. Although the ES cells positive for the targeting construct could produce chimeric animals carrying the TPH2 targeting construct (6 males and 6 females) there was no germline transmission when they were bred with C57B1/6.

Thus, we could not get germ line transmission from the positive ES cell clone (Fig. 3.44).
By RT-PCR we could show that TPH2 (but not TPH1) is strongly expressed in the testis of mice (Fig. 3.45 A). We asked the question if expression of TPH2 plays a role in spermatogenesis. To detect TPH2 expression in sperms, we isolated RNA from human sperms and could amplify a clear band of around 300 bp by RT-PCR using specific primers of human TPH2 (Fig. 3.45 B). We cloned and sequenced this fragment to confirm the result (data not shown). We could also observe a positive signal in rat spermatocytes by immunohistochemistry staining of testis sections using a TPH antibody (Fig. 3.46).

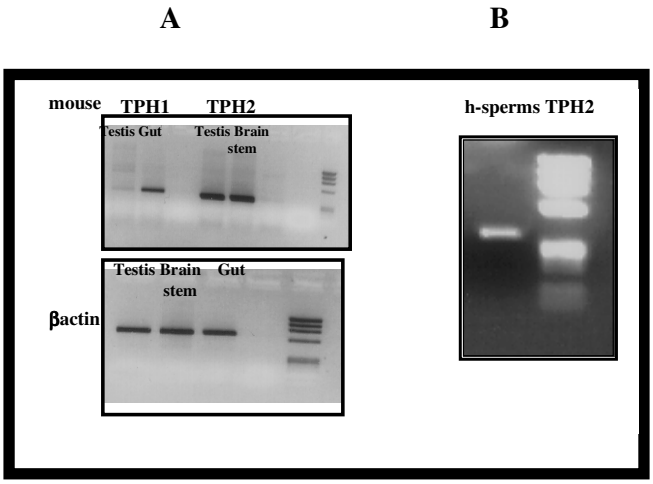

Fig. 3.45. TPH2 is expressed in mice testis, while TPH1 is not (A), also TPH2 is expressed in human sperms (B).

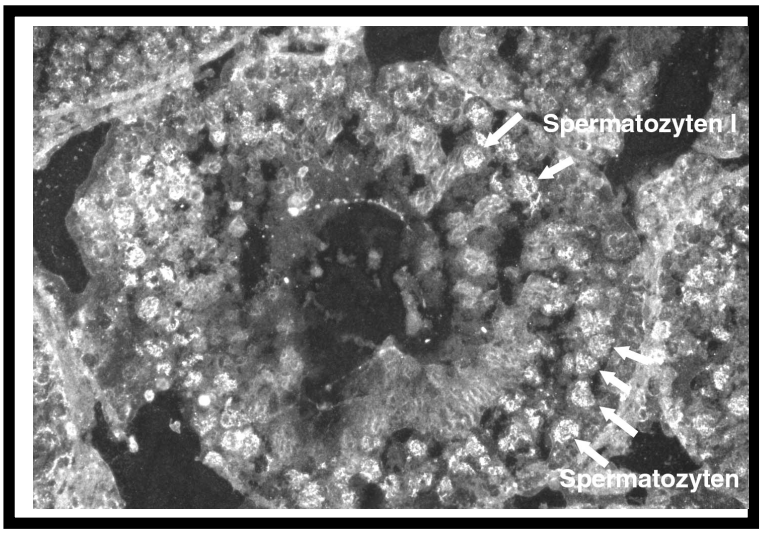

Fig. 3.46. Immunostaining of rat testis section with TPH antibodies, shows positive signals in the spermatocytes.

Then we followed the expression of TPH2 in the mice testis depending on the age using RNAse protection assay. TPH2 expression in the testis is not detected in 2 weeks old mice, and also not before puberty (2 weeks). Indeed TPH2 expression is first detectable in 3 weeks old mice, and thereafter increases continuously until they are 5 weeks old (Fig. 3.47). These results indicate that TPH2 expression correlates with spermatogenesis or sperm maturation.

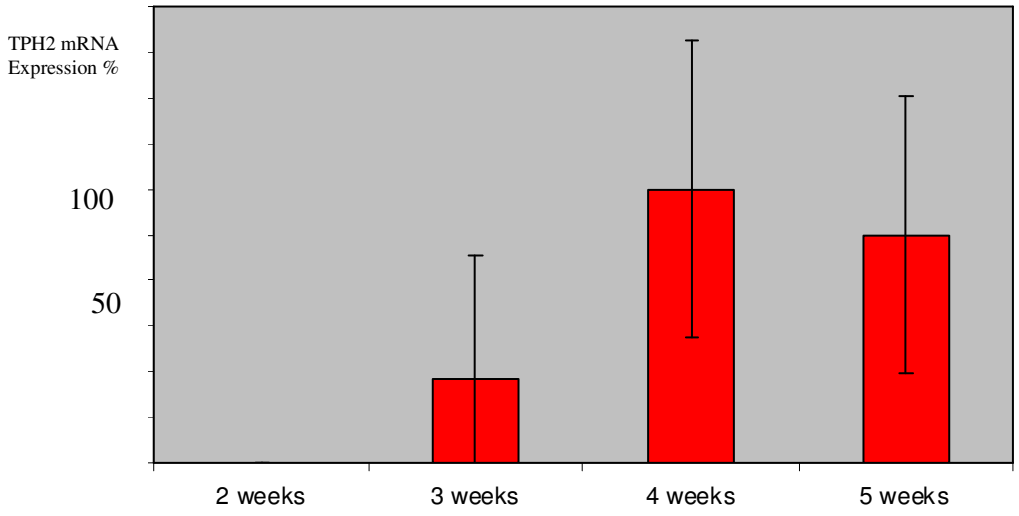

Fig. 3.47. Expression of TPH2 mRNA in testis of mice depends on the age. No TPH2 expression is detected before puberty (2 weeks old), but after that (3, 4, and 5 weeks)